AMEGHINIANA
A GONDWANAN PALEONTOLOGICAL JOURNAL

EVIDENCES OF TERATOLOGY AND MUTAGENENSIS IN PALYNOLOGICAL ASSEMBLAGES FROM THE MIDDLE TRIASSIC PUESTO VIEJO GROUP, SAN RAFAEL DEPOCENTER, ARGENTINA. IMPLICATIONS OF VOLCANISM AND REGIONAL ENVIRONMENTAL STRESS

ANA MARÍA ZAVATTIERI[1]
PEDRO RAÚL GUTIÉRREZ[2]

[1]Departamento de Paleontología, Instituto Argentino de Nivología, Glaciología y Ciencias Ambientales IANIGLA, CCT-CONICET-Mendoza, Av. Adrián Ruiz Leal s/n., Parque General San Martín, M5002IRA Mendoza, Argentina.
[2]Museo Argentino de Ciencias Naturales "B. Rivadavia" (MACN), Consejo Nacional de Investigaciones Científicas y Técnicas (CONICET), Av. Ángel Gallardo 470, C1405DJR Ciudad Autónoma de Buenos Aires, Argentina.

Submitted: 25 July 2022 - **Accepted:** 24 January 2023 - **Published:** 31 March 2023

To cite this article: Ana María Zavattieri, Pedro Raúl Gutiérrez (2023). Evidences of teratology and mutagenensis in palynological assemblages from the Middle Triassic Puesto Viejo Group, San Rafael Depocenter, Argentina. Implications of volcanism and regional environmental stress. *Ameghiniana 60*(2), 118–148.

To link to this article: http://dx.doi.org/10.5710/AMGH.24.01.2023.3533

ISSN 0002-7014
GONDWANAN PERSPECTIVES AMEGHINIANA - 2023 - Volume 60(2): 118–148

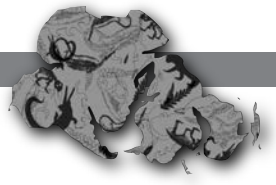

EVIDENCES OF TERATOLOGY AND MUTAGENENSIS IN PALYNOLOGICAL ASSEMBLAGES FROM THE MIDDLE TRIASSIC PUESTO VIEJO GROUP, SAN RAFAEL DEPOCENTER, ARGENTINA. IMPLICATIONS OF VOLCANISM AND REGIONAL ENVIRONMENTAL STRESS

ANA MARÍA ZAVATTIERI[1], AND PEDRO RAÚL GUTIÉRREZ[2]

[1]Departamento de Paleontología, Instituto Argentino de Nivología, Glaciología y Ciencias Ambientales IANIGLA, CCT-CONICET-Mendoza, Av. Adrián Ruiz Leal s/n., Parque General San Martín, M5002IRA Mendoza, Argentina. *amz@mendoza-conicet.gob.ar*

[2]Museo Argentino de Ciencias Naturales "B. Rivadavia" (MACN), Consejo Nacional de Investigaciones Científicas y Técnicas (CONICET), Av. Ángel Gallardo 470, C1405DJR Ciudad Autónoma de Buenos Aires, Argentina. *pedroraulgutierrez@gmail.com*

Abstract. Evidence of teratogenesis and mutagenesis documented in the palynological assemblages of the Middle Triassic Quebrada de los Fósiles Formation, San Rafael Depocenter (Mendoza, Argentina) provide an independent testimony of deteriorating atmospheric conditions at the time of sedimentation of the lower unit of the Puesto Viejo Group. Considerable explosive acid volcanism occurred during the deposition of the continental alluvial-fluvial systems of this unit, and its consequent effects on climate created stressful and adverse conditions that influenced the paleoenvironments and vegetation. To assess the degree of teratology, we characterize malformation categories for each lineage of plants represented in the dispersed palynomorphs (spores, saccate pollen, and algae) recorded in the Quebrada de los Fósiles microflora. Additionally, typical fused spores are associated with malformed tetrads, triads, and dyads which reflect reactions of the autochthonous plants (sphenophytes, ferns, bryophytes, and lycophytes) to adverse environmental conditions. Unusual morphologies are also evident in some aquatic zygospores of green algae that colonized the freshwater bodies within fluvial systems of the middle and upper sections of this unit. The palynological preparations also contain dispersed leaf cuticle fragments showing xeromorphic features that reveal mutagenetic responses of plants to paleoenvironmental stresses. The co-occurrence of morphological aberrancies observed in different lineages of palynomorphs is consistent with previous interpretations that the terrestrial and aquatic vegetation of the Quebrada de los Fósiles Formation grew in disturbed floodplain environments affected by intermittent volcanic episodes under temperate to warm seasonal arid to semiarid climatic conditions. In this contribution, we document the first clear diversity of teratological traits independently developed across different lineages of plants and possibly algae synchronously coinciding with intense explosive volcanism within the same region in the Middle Triassic.

Key words. Teratology. Mutagenesis. Palynology. Volcanism. Paleoenvironmental stress. Middle Triassic. San Rafael Depocenter. Argentina.

Resumen. EVIDENCIAS DE TERATOLOGÍA Y MUTAGÉNESIS EN ASOCIACIONES PALINOLÓGICAS DEL TRIÁSICO MEDIO DEL GRUPO PUESTO VIEJO, DEPOCENTRO SAN RAFAEL, ARGENTINA. IMPLICANCIAS DEL VULCANISMO Y el ESTRÉS AMBIENTAL REGIONAL. Evidencias de teratogénesis y mutagénesis documentadas en las asociaciones palinológicas de la Formación Quebrada de los Fósiles, Triásico Medio, Depocentro de San Rafael (Mendoza, Argentina) proveen un testimonio independiente del deterioro de las condiciones atmosféricas durante la sedimentación de la unidad inferior del Grupo Puesto Viejo. Un considerable vulcanismo ácido explosivo ocurrió durante la depositación de los sistemas aluviales-fluviales continentales de esta unidad y sus consecuentes efectos sobre el clima crearon condiciones estresantes y adversas que influyeron en los paleoambientes y en la vegetación. Para evaluar el grado de teratología identificamos categorías de malformaciones para cada linaje de planta representada en los palinomorfos dispersos (esporas, polen sacado y algas) registrados en las microfloras de la Quebrada de los Fósiles. Además, las esporas fusionadas normales se asocian con tétradas, tríadas y díadas malformadas que reflejan reacciones de las plantas autóctonas (esfenofitas, helechos, briófitas y licofitas) a condiciones ambientales adversas. Morfologías inusuales también se evidencian en algunas zigosporas de algas verdes que colonizaron los cuerpos de agua dulce dentro de los sistemas fluviales de las secciones media y superior de esta unidad. Los preparados palinológicos también contienen fragmentos de cutículas de hojas, que muestran rasgos xeromórficos que revelan respuestas mutagenéticas de las plantas al estrés paleoambiental. La co-ocurrencia de aberraciones morfológicas observadas en diferentes linajes de palinomorfos es consistente con interpretaciones previas de que la vegetación terrestre y acuática de la Formación Quebrada de los Fósiles creció en ambientes fluviales y de planicie de inundación afectados por episodios de actividad volcánica intermitente bajo condiciones climáticas templadas estacionales áridas a semiáridas. En esta contribución documentamos la primera evidencia clara de rasgos teratológicos desarrollados independientemente en diferentes linajes de plantas y posiblemente algas, coincidiendo sincrónicamente con el intenso vulcanismo explosivo dentro de la misma región en el Triásico Medio.

Palabras clave. Teratología. Mutagénesis. Palinología. Vulcanismo. Estrés paleoambiental. Triásico Medio. Depocentro San Rafael. Argentina.

THE COMPOSITION OF FLORA is directly related to the environmental and climatic conditions in the area where the plants live. Land vegetation can provide insights into ecosystem health in the fossil record. In particular, plants can uniquely indicate paleoenvironmental stresses by leaving behind structural malformations in their spores and/or pollen under conditions such as heightened radiation and chemical pollutant exposure (Visscher *et al.*, 2004; Foster & Afonin, 2005; Bazhina *et al.*, 2007; De Storme & Geelen, 2013; Benca *et al.*, 2018, 2022; Lindström *et al.*, 2019; Chu *et al.*, 2021; Looy *et al.*, 2021). Several studies have shown that volcanism is a critical factor for long-term climate change, and global warming is widely regarded to have contributed to numerous past biotic crises (Sun *et al.*, 2012; Payne & Egan, 2019; Chen & Xu, 2019).

Volcanic eruptions inject a wide range of gases into the atmosphere. Sulfur dioxide (SO_2), carbon dioxide (CO_2), and methane (CH_4) are volumetrically the most significant greenhouse volcanic gases that caused warming over geological time. Massive volcanism due to large igneous provinces has been associated with several mass extinction events, but individual large explosive volcanoes can also cause regional to global environmental perturbations beyond climate change (Williams *et al.*, 1992; Wignall, 2001, 2005; Ward, 2009; Black *et al.*, 2012, 2014; Grasby *et al.*, 2013, 2019; Spalletti & Limarino, 2017; Osipov *et al.*, 2020; Racki, 2020; Cui *et al.*, 2021; Font *et al.*, 2022; Shen *et al.*, 2022). Kutterolf *et al.* (2013) suggest that large explosive volcanoes can inject appreciable enough volumes of bromine and chlorine into the atmosphere, substantially depleting the stratospheric ozone layer on a regional scale. Cadoux *et al.* (2015) demonstrate that explosive volcanism can induce ozone holes, and Black *et al.* (2014) also discussed how volcanoes can induce regional-scale acid rain.

Phytotoxic volcanic emissions and radiation stress can cause abnormalities in plants and malformed spores and pollen (sporomorphs), and tetrad formation (Mičieta & Murín, 1996; Visscher *et al.*, 2004, 2011; Foster & Afonin, 2005; Yin *et al.*, 2014; Hochuli *et al.*, 2017; Benca *et al.*, 2018, 2022; Benton, 2018; Lindström *et al.,* 2019; Grasby *et al.*, 2020; Chu *et al.,* 2021). Multiple malformations have been shown to be associated with environmental stress. However, some types of morphological alterations are not suitable for environmental stress detection as they do not require stress to form, such as ordinarily unseparated spore tetrads in some arid land lycophytes, unseparated tetrads of *Classopollis* pollen grains, or the pollen of the rare plant species that naturally produce trisaccate grains. Thus, abnormal spores and pollen grains can also be attributed to the effects on plants of extremely adverse environmental conditions generated or not by volcanism (Gupta & Devi, 1994; Tiwari & Meena, 1989; Visscher *et al.*, 2004; Foster & Afonin, 2005; Ram-Awatar, 2011; Saxena *et al.*, 2015; Hochuli *et al.*, 2017; Benca *et al.*, 2018; Stukins, 2022).

High frequencies of sporomorph malformations associated with increased exposure to UV-B radiation and heavy metal poisoning have been widely observed in sediments deposited contemporaneously with large igneous provinces (LIPs). These LIPs were the trigger for environmental stress associated with strong climatic changes and extinction events, the most severe of which were recorded across the Permian–Triassic transition and at the end of the Triassic (Looy *et al.*, 2001, 2005; Visscher *et al.*, 2004; McGhee *et al.*, 2013; Kürschner *et al.*, 2013; Hochuli *et al.*, 2017; Lindström *et al.,* 2019; Fijałkowska-Mader, 2020; Marshall *et al.*, 2020; Chu *et al.*, 2021).

Lindström *et al.* (2019) differentiated between non-mutagenic and mutagenic aberrant spores and/or pollen grains. Non-mutagenetic abnormalities can be induced through various environmental stresses (*e.g.*, drought, water logging, temperature changes, etc.), causing morphological malformations (teratology) of the reproductive cells. The term "teratology" describes developmental deviations or abnormal/aberrant patterns, which may indicate various forms of environmental stress that limit a plant's growth, development and/or physiological processes of a plant. In many cases, the environmental stress is seasonal, and it should be distinguished from anomalous environmental stresses (*e.g.*, elevated UV-B radiation exposure, regional acid rain near volcanoes, heightened mercury and/or heavy metal deposition). Seasonal environmental stress may only affect parts of a plant population resulting in a variable amount of immature (premature shedding) spores or pollen that may or may not still be retained in tetrads when found dispersed. Mutagenic changes (=genetic alterations) produced in the mother plant, lead to an increase in the number of spores or pollen grains that are aberrant and non-viable. Malformation traits can be produced through meiotic deviations

(mutations) and deviations later in the sporogenesis process (tetrad/free spore stage). Both of these traits can occur within sporomorphs, and some give clues into which developmental processes were disrupted" (*e.g.,* Benca *et al.*, 2022). Recent works have shown that elevated UV-B radiation increases malformations in pine pollen and that the resulting teratology has the same characteristics as those recorded in gymnosperm bisaccate pollen during the end–Permian (Benca *et al.*, 2022, and references therein).

During the Permian and Early Triassic, central western Argentina manifested an active volcanism related to the Choiyoi extensional igneous province (Kay *et al.*, 1989; Llambías *et al.*, 1993; Llambías & Sato, 1995; Rocha-Campos *et al.*, 2011; Spalletti & Limarino, 2017), that continued during the deposition of the Triassic Puesto Viejo Group (Kleiman & Salvarredi, 2001; Kleiman & Japas, 2009; Monti & Franzese, 2016, 2019). The Middle Triassic was characterized by episodes of extensional rifting manifested by intense explosive volcanic activity. Rhyolitic pyroclastic flow deposits, andesitic lavas, basaltic intrusives, and volcaniclastic facies reveal intense volcanism coeval with the deposition of the Quebrada de los Fósiles Formation (QdlF Fm), lower unit of the Puesto Viejo Group, San Rafael Block, Mendoza Province (Monti, 2015; Monti & Franzese, 2016, 2019). Sedimentological data suggest that the vegetation recorded from this unit grew in fluvial systems while profuse volcanic activity introduced large volumes of ash and the emission of large amounts of greenhouse (thermogenic) gases into the atmosphere (Spalletti *et al.*, 2003; Monti & Franzese, 2016, 2019; Spalletti & Limarino, 2017; Cariglino *et al.*, 2018; Zavattieri *et al.*, 2020), with consequent effects on climate (resulting in generalized regional aridity) and paleoenvironments that directly influenced the development of plant communities.

Here, we describe and characterize quantitatively the teratology categories observed in spores and pollen produced by different lineages of plants and algae recorded in palynological samples from the Middle Triassic QdlF Fm succession in the San Rafael Depocenter. We discuss contemporaneous volcanism and the implications on climate as causality of the co-occurring evidences of teratologies described in this paper.

Institutional abbreviations. IANIGLA, CCT-CONICET-MENDOZA, Instituto Argentino de Nivología, Glaciología y Ciencias Ambientales, Centro Científico Tecnológico - Consejo Nacional de Investigaciones Científicas y Técnicas, Mendoza, Argentina; **MACN,** Museo Argentino de Ciencias Naturales "Bernardino Rivadavia", Ciudad Autónoma de Buenos Aires, Argentina; **MPLP,** Mendoza Paleopalinoteca-Laboratorio de Paleopalinología; **BAPal,** Buenos Aires Palinología.

GEOLOGICAL SETTING

The San Rafael Depocenter (Ottone *et al.*, 2014), also referred as the San Rafael Sub-basin by Monti and Franzese (2016) or the San Rafael Block (Monti, 2015; Monti & Franzese, 2016; Cariglino *et al.*, 2018) is geographically located in the southwest of Mendoza Province, Argentina (Fig. 1). It crops out marginally as a small isolated depocenter to the south-southwest of the Cuyana Basin, with which it shares a part of the Triassic tectonic rift phases (Monti & Franzese, 2016, 2019). The complete stratigraphy and origin of the units comprising the San Rafael Depocenter have been summarized by Domeier *et al.* (2011), Ottone *et al.* (2014), and Monti and Franzese (2016, 2019). The continental Triassic infilling of the San Rafael depocenter comprises sedimentary and volcanic deposits of the Puesto Viejo Group (Stipanicic *et al.*, 2007). A basal unconformity, attributed to the Huárpica diastrophic phase (López Gamundí *et al.*, 1989), separates the Permian Cerro Carrizalito Formation from the Triassic Puesto Viejo Group (Ottone *et al.*, 2014) and/or unconformably overlies volcanic rocks of the upper Choiyoi Group (Middle Permian–Lower Triassic) (Kleiman & Salvarredi, 2001; Kleiman & Japas, 2009; Monti & Franzese, 2016; Irmis *et al.*, 2022). It is overlain unconformably by the Paleogene Aisol Formation and/or Quaternary deposits (González Díaz, 1972).

The Puesto Viejo Group consists of alluvial and fluvial sequences interbedded with rhyolitic pyroclastic flows (ignimbrites), andesitic lavas, shallow basaltic intrusives and abundant tuff deposits of bimodal magmatism (González Díaz, 1964; Spalletti, 1994; Kokogián *et al.*, 1999, 2001; Kleiman & Salvarredi, 2001; Monti, 2015; Ottone *et al.*, 2014; Monti & Franzese, 2016). It includes two units, the lower QdlF Fm and the upper Río Seco de la Quebrada Formation (RSdlQ Fm) (Stipanicic *et al.*, 2007). The basal part of the QdlF Fm is characterized by debris-flow deposits, mainly composed of coarse-grained epiclastic strata related to proximal alluvial-fan systems located to the basin border

faults. These basal deposits were eventually covered by pyroclastic flows (lower ignimbrite). Finer-grained strata of the QdlF Fm were extensively deposited towards the center of the basin and represent fluvial systems characterized by channel-fills and floodplain deposits, also interrupted by pyroclastic flows (upper ignimbrite) and intrusive volcanic rocks. The uppermost ignimbrite level marks the boundary with the overlying RSdlQ Fm. The RSdlQ Fm begins with coarse-grained sediments due to reactivation of internal faults, interpreted as braided to low-sinuosity meandering fluvial systems. Towards the upper part of the unit, coarse-grained strata represent the distal sections of alluvial fans and are covered by lava flows (Monti & Franzese, 2016, 2019).

The QdlF Fm, in its type section (Fig. 2.1), begins and ends with pyroclastic flow (ignimbrite) deposits, both of which have been radiometrically dated. The age of the basal ignimbrite gave 243.9±2 Ma by LA-ICPMS U–Pb geochronology (Monti *et al.*, 2018), and the upper ignimbrite 235.8±2 Ma by U–Pb zircon SIMS analyses (Ottone *et al.*, 2014). Accordantly, the QdlF Fm accumulated from the Middle (Anisian) to the earliest Late (early Carnian) Triassic, and the RSdlQ Fm was deposited during the early Late Triassic (Cohen *et al.*, 2013; updated) (Fig. 2). Recently, Irmis *et al.* (2022) analyzed previous radiometric data of the Puesto Viejo Group and recalculated the ages of the basal and upper pyroclastic flow deposits of the QdlF Fm, indicating ages of 243.5±11.8 Ma and 235.8±8.8 Ma, respectively, with mean uncertainties of *ca.* ±12 Ma and *ca.* ±9 Ma. According to these data, recently Mancuso *et al.* (2021) and Pedernera *et al.* (2022) recently placed the QdlF Fm in the Early to Middle Triassic, and more precisely they constrained the age of the lower unit of the Puesto Viejo Group to Middle Triassic (mid-?upper Anisian to ?mid-?late Ladinian) (see Pedernera *et al.*, 2022, tab. 1) and the RSdlQ Fm to Middle Triassic (?mid-?late Ladinian) to early Late Triassic (?early Carnian) (see Pedernera *et al.*, 2022, fig. 2).

Middle Triassic fossil plant and palynological assemblages of the Puesto Viejo Group have been recorded, up to now, only from the QdlF Fm (Ottone & García, 1991; Vázquez, 2013; Ottone *et al.*, 2014; Coturel *et al.*, 2016; Cariglino *et al.*, 2018; Zavattieri *et al.*, 2020; Gnaedinger *et al.*, 2020; Gutiérrez & Zavattieri, 2021).

The Quebrada de los Fósiles Formation type section

The type section of the QdlF Fm crops out at the homonymous creek and represents the lower part of the Puesto Viejo Group (Figs. 1.3, 2.1). The type section is more than 200 m thick and is characterized by epiclastic and volcaniclastic layer, profuse air fall tuffs, rhyolitic pyroclastic flow deposits at the base and top, and basaltic intrusives (Fig. 3.1–3.2). Spalletti (1994), Monti (2015), Monti and Franzese (2016), and Cariglino *et al.* (2018) provided a detailed litho-sedimentological description of the type section defining two main depositional environments: 1) high sinuosity river system (traction-load dominated deposits) with a typical fining-upwards arrangement and deposits of discharge during flooding events. It includes main channel deposits, sandbars associated with channels, crevasses attributed to discharge channels, and crevasse splay deposits; 2) floodplain facies (decantation-dominated deposits) mainly integrated by fine sediments of thick tabular deposits generated by subaqueous decantation (suspension-load deposits), laterally intergraded with shallow water bodies, locally with incipient development of paleosols and thin limestone levels with stromatolite-like structures. Lacustrine horizons contain abundant microspores, silicified megaspores, ostracods and spinicaudatan valves; insect remains, and few fish scales (Tassi *et al.*, 2013; Cariglino *et al.*, 2018; Zavattieri *et al.*, 2020). The pyroclastic flow deposits at the base and top of the type section, the common presence of tuffs and tuffaceous sediments of the floodplains, and the basaltic intrusives within the succession evidence intense volcanism coeval with the deposition of the QdlF Fm (Fig. 3.1–3.3).

Plant remains (megaflora and microflora assemblages) were recovered from three sectors of the type section of the QdlF Fm cropping out at the homonymous creek (Figs. 1.3, 2.1, 3.1–3.3): a) thin tabular tuffaceous shales with abundant organic matter (AMZ2 section of the integrated type profile; Figs. 1.3, 2.1, 3.1); b) tuffaceous shales and limestones with light grey to whitish shales having fine and densely distributed root casts indicating the development of incipient paleosols (AMZ1 section of the integrated type profile; Figs. 1.3, 2.1, 3.1), and c) tabular deposits of laminated siltstones interbedded with light yellow-orange bio-laminated calcareous layers (GzD section of the integrated type profile, Figs. 1.3, 2.1, 3.1).

The Quebrada de los Fósiles Formation at Río Seco de la Quebrada section

Monti (2015), Vázquez (2013), and Monti and Franzese (2016) described the QdlF Fm outcropping at the southern Río Seco de la Quebrada Creek (Figs. 1.3, 2.2). The base of the QdlF Fm is marked by a border-fault that separates the Permian basement from the Triassic unit. The top of the section is transitional to RSdlQ Fm. Distinctive features of the outcrops of the QdlF Fm in this creek are an almost flat topographic relief with a slight inclination to the east and strong faulting. Thus, the sedimentary profile of the unit in this creek is composed of dismembered and partial sections (see Monti & Franzese, 2016). The QdlF Fm starts with coarse and thick alluvial-fan deposits. Upwards, the low-sinuosity gravel river system is truncated by a vesicular andesitic basalt mantle (Fig. 2.2). The section above the intrusive basalt is characterized by low-energy deposits, consisting of a floodplain with minor high-sinuosity meandering channels with crevasse splays, crevasse channels, and/or isolated small discharge channel sand local shallow lacustrine and/or palustrine deposits. Floodplain facies are represented by massive and laminated greenish-gray mudstones, siltstones, and tuffaceous mudstones with inter-bedded organic-rich horizons and poorly preserved plant remains. Local development of paleosols is evidenced by fine and dense root-cast. Local shallow lacustrine deposits are characterized by grayish-green to very light-gray shale banks with thin limestone levels of relatively stable water bodies. In the Río Seco de la Quebrada section (Fig. 3.4), the palynological samples for this study were

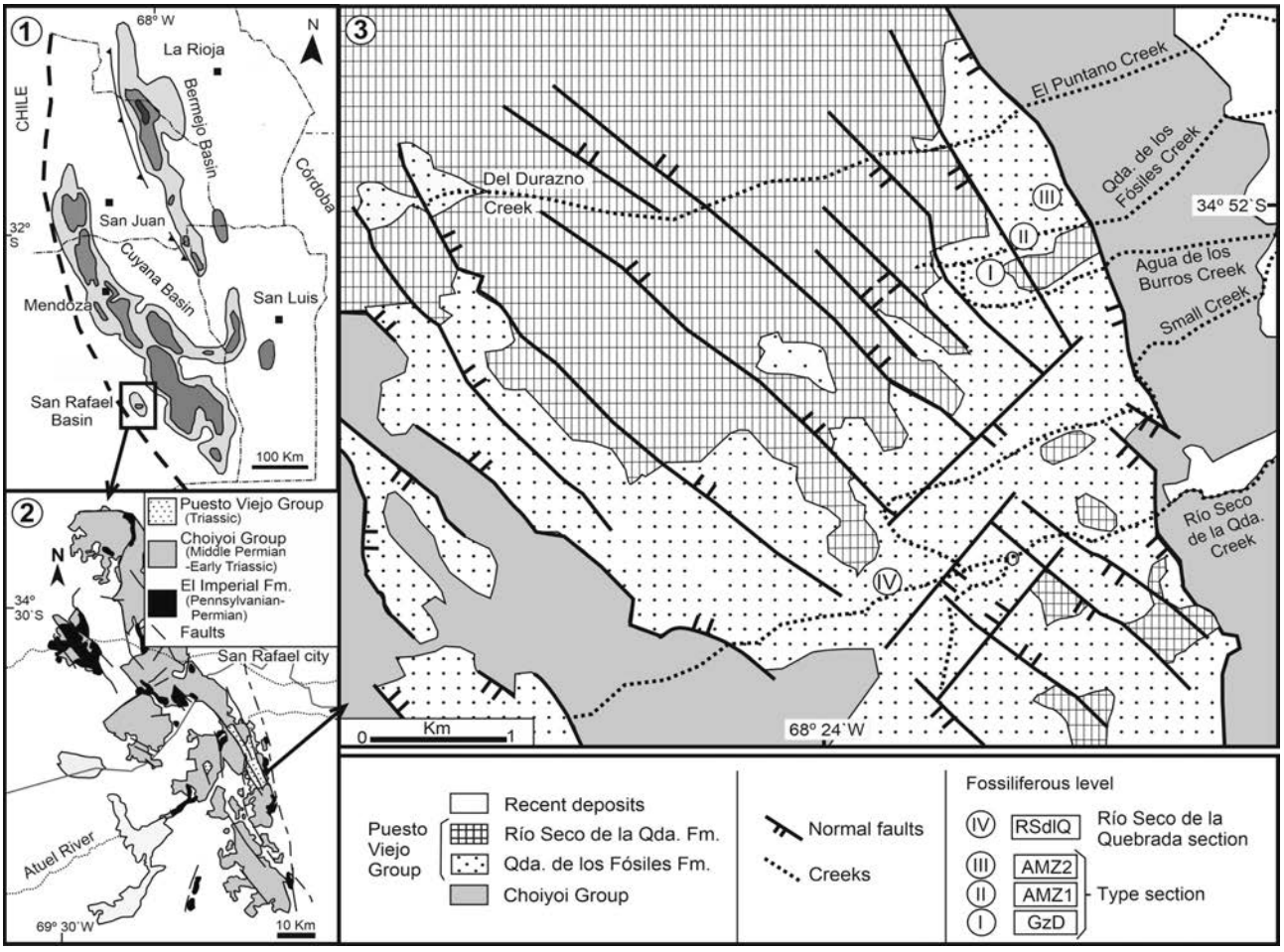

Figure 1. Geological map (modified from Zavattieri *et al.,* 2020). **1,** Distribution of the Triassic basins in central-western Argentina, showing the location of the San Rafael Depocenter; **2,** outcrops of the Puesto Viejo Group in the San Rafael depocenter; **3,** geological map of the Puesto Viejo Group in the study area and locations of the studied sections in the Quebrada de los Fósiles Creek: I, GzD; II, AMZ1; III, AMZ2 (see Fig. 2) and IV, location of the studied levels in the section Río Seco de la Quebrada Creek; Qda: Quebrada; Fm: Formation.

taken from grey bentonitic claystones, thin dark-brown to black carbonaceous shales (coal levels) with abundant organic plant debris and from grey thin laminated siltstones with common organic plant debris (Fig. 3.5–3.10), interpreted as swamps, marginal lacustrine bodies, stagnant pools, moist soils, and thin peat levels of floodplain subenvironments.

MATERIALS AND METHODS

The palynological fossil materials of the QdlF Fm, Puesto Viejo Group were obtained from 22 levels of the QdlF Fm type locality exposed on the homonymous creek and from 17 levels of the Río Seco de la Quebrada Creek (Fig. 2). The samples were processed following standard palynological extraction techniques, which included treatments with HCl-HF-HCl acids, and when required, two minutes of oxidation with concentrated nitric acid (HNO_3). Details of palynological techniques, catalog number of samples, and used microscopic equipment have been detailed in Zavattieri *et al.* (2020) and Gutiérrez and Zavattieri (2021). The QdlF Fm microflora yields abundant, well-preserved, and diverse spores, pollen, freshwater algae, fungi, and other organic-walled tissues (Supplementary Online Information 1—SOI 1—). Aberrant palynomorphs and exceptionally abundant unseparated spores and pollen grains were found during the study and quantitative analysis of the QdlF Fm assemblages.

To assess the percentage of aberrant forms, all normal and aberrant specimens of spores and pollen grains were counted separately. Only specimens that exhibited clear signs of aberrancy were counted as abnormal sporomorph type (teratology type). The teratology categories were based on five different groups/lineages of plants identified in the

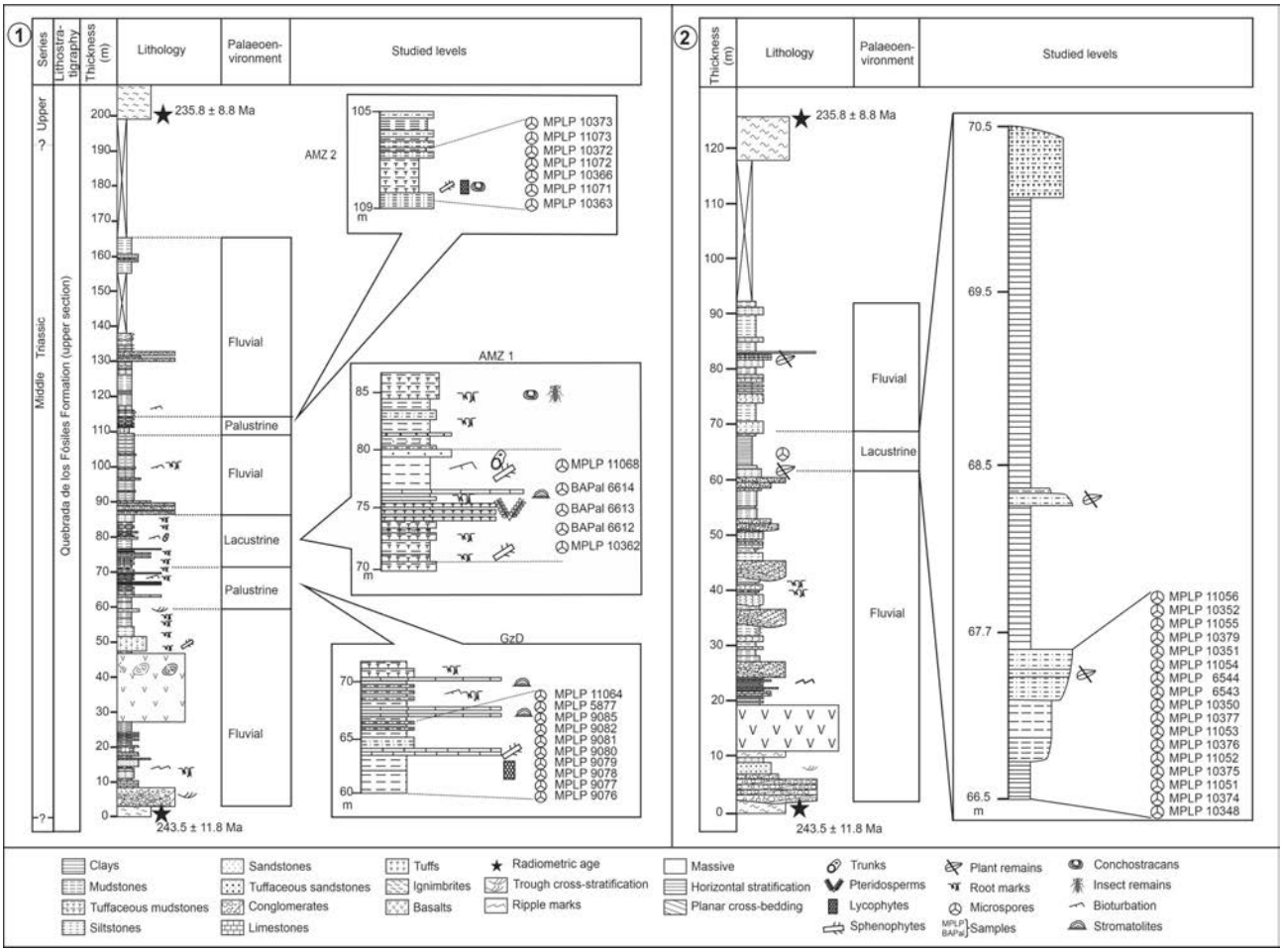

Figure 2. Sedimentological section of the Quebrada de los Fósiles Formation cropping out at: **1,** Quebrada de los Fósiles Creek; **2,** Río Seco de la Quebrada Creek indicating the litho-sedimentological characteristics and fossil levels and the location of the studied palynological samples, stars show sample dating levels of the basal and top effusive levels of the type section (Fig. 1; modified from Zavattieri *et al.,* 2020).

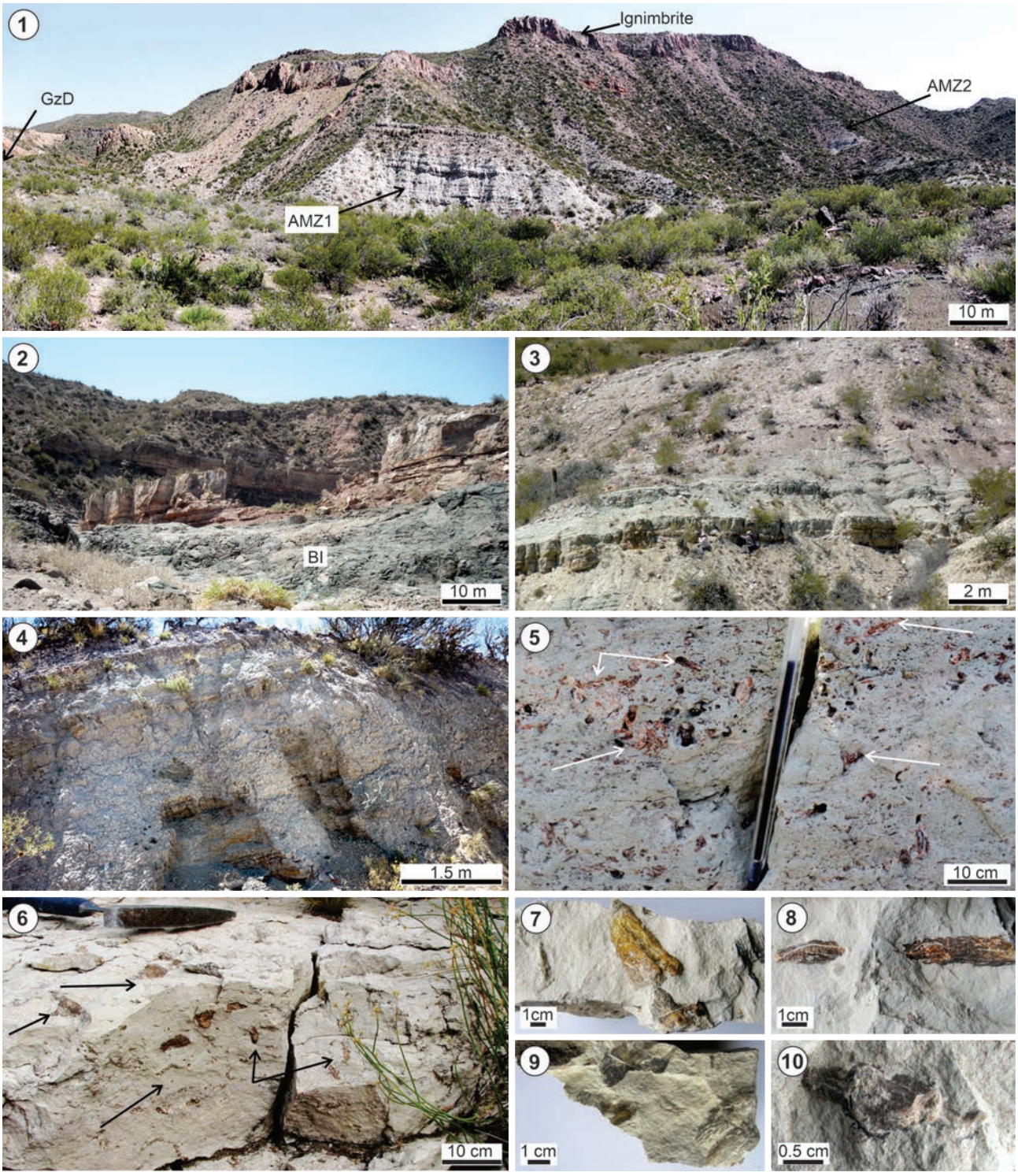

Figure 3. Photographs of the deposits of the Quebrada de los Fósiles Formation; **1,** panoramic view of the type locality; **2,** intrusive basalt (BI) concordant with sedimentary strata outcropping in the Río Seco de la Quebrada Creek section; **3,** view of the GzD section at the Quebrada de los Fósiles Creek section, note grayish tuffaceous strata which contain lycopsids and sphenopsids plant remains and palynological assemblages; **4,** tuffaceous (bentonitic) fine-grained and thin coal levels yielding sphenophyte remains and palynological studied assemblages at the section at the Río Seco de la Quebrada Creek; **5–6,** tuff levels containing abundant sphenophyte fragments (arrows) outcropping in the Río Seco de la Quebrada Creek; **7–10,** details of identified sphenophyte fragments dispersed in tuff levels.

palynological assemblages: Sphenophytes/Equisetales (*Calamospora*), Lycophytes (mainly *Aratrisporites* and cingulizonate spores), Bryophytes + true ferns (smooth and apiculate trilete spores with triangular and/or circular contour), gymnosperm pollen grains (smooth and striate monosaccate and bisaccate pollen and plicate grains), and chlorophytic alga zygospores/aplanospores. Six hundred specimens were counted for each group (maximum two slides per level) following the criteria of Benca *et al.* (2022), who pointed out that from that number of specimens, no significant changes were detected in the counts in herbarium specimens. Specimens with more than one teratological feature (*i.e.*, bisaccate grains with asymmetric sac/s plus a protosac on the central body; spores with cracked exine and asymmetric leasura rays, etc.) were counted for each teratological category. In the analyzed samples (Supplementary Online Information 2 —SOI 2—), there are palynological assemblages with markedly dominant groups, like in the lower part of the QdlF section (MPLP 9076 to MPLP 9082) where Chlorophytic zygospores exceed 85% of the assemblages (SOI 1), whereas the other lineage of plants does not reach the minimum of 100 specimens counted. Similarly, in the sample MPLP 11068 of the same profile, the "true ferns + Bryophytes" group reaches more than 90% of the microflora (SOI 1). A group of samples shows palynological assemblages dominated by Equisetales and/or Lycophyte spores (SOI 2), whereas remaining lineages of spores are scarcely present (less than 100 specimens counted), although also included in the analysis (SOI 3).

Within spores (true ferns, bryophytes, and lycophytes), two large groups were discriminated: the phenotypically normal forms that can appear isolated/dispersed or grouped (dyads, triads, tetrads, and clusters) and the abnormal spore types/traits in which some of the categories of Lindström *et al.* (2019) were identified: a) dwarf spores —and giant spores, herein recorded as abnormal oversized spores—, b) asymmetrical laesura (=uneven trilete rays), c) cracked exine and/or aberrant folding, d) spores with thickened labra or labra with growths, d) deformed outline, and f) weakly deformed proximal area. Within Equisetales spores (*Calamospora*), dispersed and/or fused normal spores (dyads, triads, tetrads) and aberrant ones were distinguished. These last include dwarfed and unexpanded specimens, dispersed or integrating tetrads (having one or more dwarfed and/or unexpanded forms) which were considered as a counting unit. Because folded, broken, or obscured specimens were always counted as normal, the obtained aberrancy values may be an underestimation.

Gymnosperm pollen grains bearing two "normal size and shape" sacci were counted as phenotypically normal. For teratology categories in bisaccate grains, we follow the malformation types proposed by Benca *et al.* (2022, p. 3. fig. 1), which are here extended to taeniate/striate bisaccate pollen grains. These include: a) grains with asymmetrical sacci; b) an atypical number of sacci; c) conjoined grains (dyad, triad, tetrad); d) oversized (giant) grains —and/or undersized (dwarf) grains recorded in these assemblages—; and, e) unseparated grains (=grouped or aggregates). In monosaccate pollen (smooth and/or taeniate/striate grains), the presence of a "symmetrical/not indented, etc." sac was counted as a normal condition. In the studied assemblages, we have also identified bisaccate and monosaccate grains (smooth or taeniate grains) having protosacs and/or protuberances in the central body, strongly lobed monosaccate grains or those with a markedly sinuous margin that appear to be polysaccates, aberrant striations and/or aberrant thickening, which were herein considered as clearly pollen malformations types and counted as teratology categories. Additionally, because a single pollen grain can exhibit multiple abnormalities, the occurrence of each malformed type was scored independently to determine the frequency of specific malformation categories.

Chlorophytic algae are represented by normal zygospores or aplanospores (dispersed and/or forming clusters) and aberrant forms, mainly observed in the genus *Ovoidites*.

This study includes observations of teratological traits in the cuticle remains that appear dispersed in the palynological preparations. They do not appear in significant quantities to be included in the counts. They are just described qualitatively as additional independent teratological evidence.

The Tillia 2.6.1 by Grimm, 1991-2019 programs were used for graphic data.

RESULTS

Although the phenotypically normal forms dominate the miospore assemblages of the QdlF Fm microflora (SOI 2; Fig. 14), morphological malformations (teratologies) are observed co-occurring in different lineages of dispersed vascular plant spores and pollen, chlorophytic algae representatives, as well as in some palynological cuticle fragments.

Equisetales. The Equisetales (Sphenophytes) are producers of *Calamospora* spores (Figs. 5, 6.1–6.4, 8.1–8.12), which is one of the dominant genera recorded in the QdlF Fm palynological assemblages (*ca.* 25.1% in the Río Seco de la Quebrada section; *ca.* 7.7% in Quebrada de los Fósiles section; Fig. 4, SOI 1).

The aberrant spores of *Calamospora* exhibit at least one of the following teratological features defined by Lindström *et al.* (2019, p. 4, table 1): minute size (dwarfed forms), unexpanded forms, aberrant folding, labra thickened or with growths, uneven trilete rays or combination of one or more of these teratologies. Some of these teratological traits are illustrated and/or exemplified in Figs. 6.1–6.4, 8.10–8.12. These malformations appear in the dispersed spores and/or in their tetrads, triads, and dyads, which can include at least one of mentioned aberrant spores (Figs. 5.4–5.13, 5.18–5.29, 8.1–8.2, 8.4–8.5, 8.7). Normal tetrads (Fig. 5.1–5.3) are commonly associated with malformed ones in the studied material. They include tetrads with various-sized spores (dwarf and/or giant) (Fig. 5.4–5.9), reduced or unequal number of spores (Figs. 5.10–5.13, 5.26–5.29; 8.1–8.5), fused dyads (Figs. 5.14–5.17, 5.20–5.25, 8.6–8.8), and others characterized by at least one of the individual spores being morphologically deformed or aberrant (Fig. 5.8–5.9), and/or deformed or fused tetrads or dyads (Fig. 5.18–5.19), most of which are non-functional spores.

Teratology in *Calamospora* appear well represented in both studied sections: in the Río Seco de la Quebrada section, they are present in all samples varying between 4.0% (MPLP 6544) and 35.0% (MPLP 10374) (SOI 2, Fig. 14). In the Quebrada de los Fósiles section they are observed in 16 of the 22 levels analyzed, ranging between 2.0% (MPLP 9877) and 47.0% (MPLP 11071) (SOI 2, Fig. 14).

Lycophytes. Spores derived from Lycophytes are rare to common constituents of the type section, ranging from 0.3% (MPLP 9082) to 90.1% (MPLP 11071), as well as in the Río Seco de la Quebrada section: 0.8% (MPLP 10351) to 88.4% (MPLP 10377) of the total assemblages (see SOI 1, Fig. 4). Phenotypically abnormal Lycophyte spore genera (Pleuromeiales: *Aratrisporites;* and Selaginellales: *Densoisporites, Carnisporites, Secarisporites*) (SOI 2, Fig. 14) are present variably in both sections: 0.5% to 15.2% in the Río Seco de la Quebrada section, and 0.2% and 4.7% in the Quebrada de los Fósiles section. Among aberrant forms of these lineages, dwarf spores (1.7–6.0% in the Río Seco section of the Quebrada; 0.3–1.0% of the Quebrada de los Fósiles), and spores having aberrant folding and/or cracking exine have been mainly identified (0.3–14.5% in the Río Seco section of the Quebrada; 0.2–4.0% of the type section (SOI 2). Remarkably, among lycopsid spores, fused specimens (dyads, triads, tetrads, and clusters; examples in Figs. 7.1–7.18, and Figs. 8.14–8.17) are quite common in some levels: in the Río Seco of the Quebrada section ranging between 0.7% to 46.3%, and less frequent in the Quebrada de los Fósiles section (0.7–9.8%) (SOI 2).

True ferns and Bryophytes. Triangular and circular laevigate spores are scarce to common through the QdlF assemblages in both sections (Fig. 4, SOI 1). True fern + Bryophyte spores (SOI 2, Fig. 14) with evidence of teratology are evident in the 17 levels analyzed in the Río Seco de la Quebrada section with values ranging from 5.0% (MPLP 10352) and 62.8% (MPLP 6544). In the Quebrada de los Fósiles section, these dispersed spores are recorded in 15 of the 22 analyzed samples, with values ranging from 2.7% (BAPal 6613) to 56.0% (MPLP 9977).

Some of the circular to triangular trilete spores show the following abnormal features in their morphology, considered aberrant forms based on Lindström *et al.* (2019, fig. 2, tab. 1):

a) Spores with aberrant folding (exines with transverse folds) (examples in Fig. 6.8–6.10, 6.12–6.14) and/or cracks in the exine (examples are shown in Fig. 6.5, 6.7–6.10, 6.12–6.14) are features that may indicate genetic disturbance. In the Quebrada de los Fósiles section (SOI 2), these malformed forms appear in 11 of the 22 analyzed levels, ranging between 2.2% (BA Pal 6613) to 23.3% (MPLP 9085). In the Río Seco de la Quebrada section (SOI 2), aberrant folding observed in true fern + bryophyte spores are represented by 0.3% (MPLP 11055) and 12.3% (MPLP 6543).

b) Spores with a weakly deformed proximal area (Fig. 6.23–6.24) are present in 6 of the 15 samples from the Quebrada de los Fósiles section (SOI 2), with values ranging from 0.8% (MPLP 11073) and 54% (MPLP 9077). In contrast, in the Río Seco de la Quebrada section (SOI 2) they appear in low proportions in 4 of the 17 samples studied, with variable proportions: 0.3% (MPLP 6544) and 1.3% (MPLP 11051).

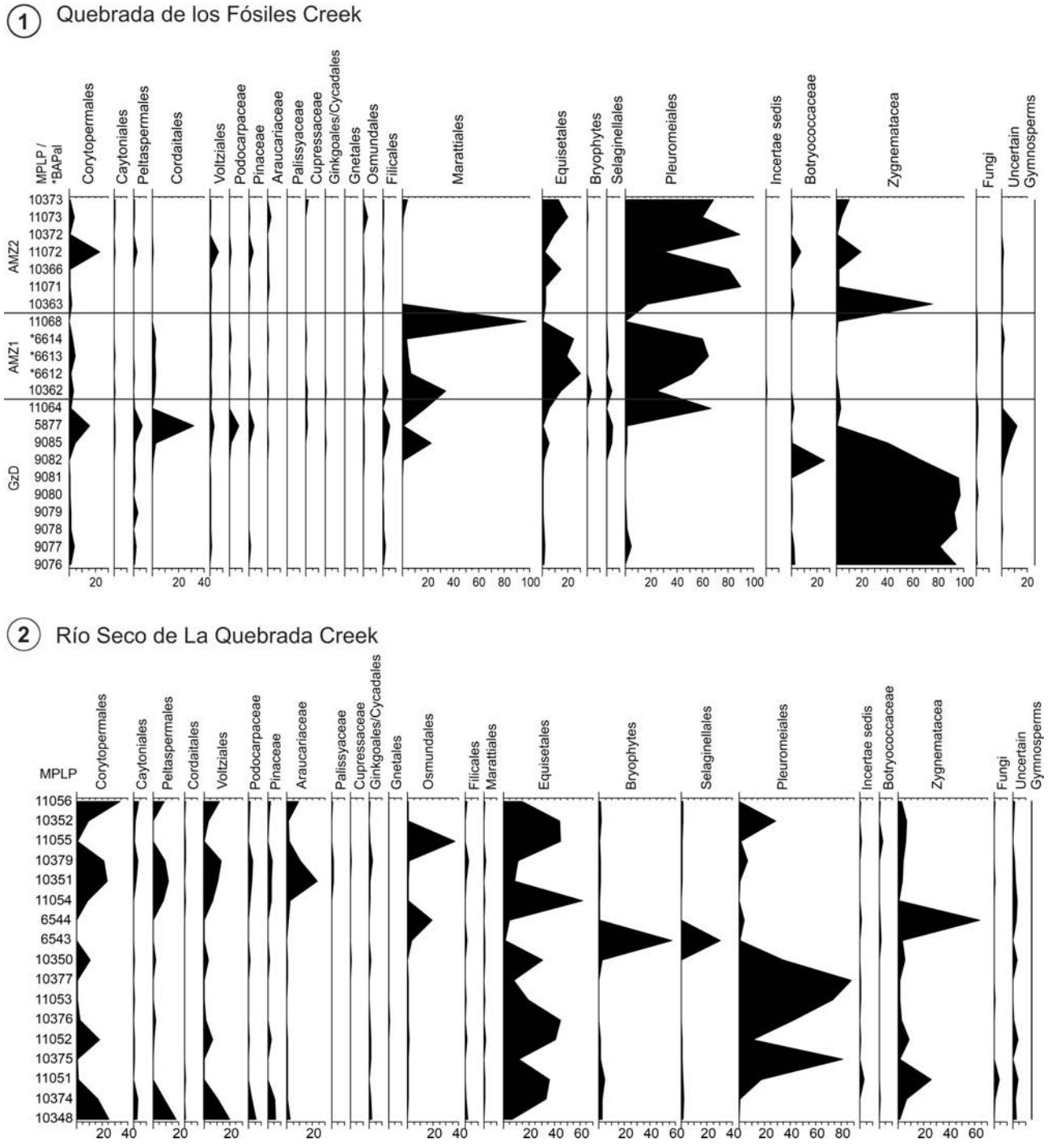

Figure 4. Composition and distribution (in %) of dispersed miospore and their botanical affinities representation recorded in the Quebrada de los Fósiles Formation, Puesto Viejo Group.

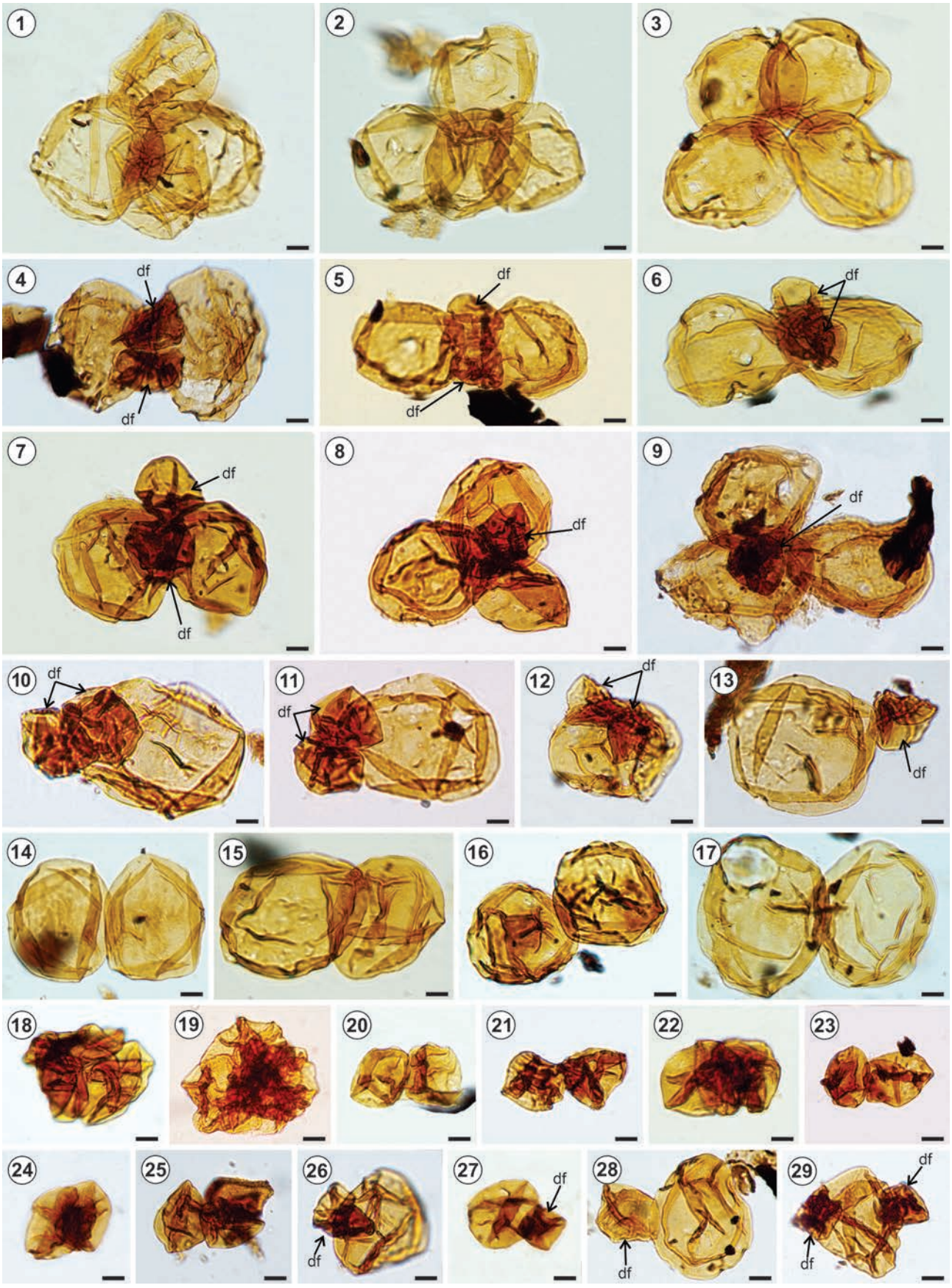
1
2
3
4
df
df
5
df
df
6
df
7
df
df
8
df
9
df
10
df
11
df
12
df
13
df
14
15
16
17
18
19
20
21
22
23
24
25
26
df
27
df
28
df
29
df
df

c) Dwarfed forms (Figs. 6.20, 6.25–6.26; 9.2–9.3, 9.6, 9.8–9.9, 9.12, 9.14, 9.17, 9.19) distinguished from normal spores (Figs. 6.21–6.22, 9.1, 9.4, 9.7, 9.10–9.11, 9.15–9.16, 9.18–9.19) by significant smaller size, but identical morphology of known species. In the Río Seco de la Quebrada section, they appear in all 15 of the levels analyzed with values between 0.3% (MPLP 11055) and 11.3% (MPLP 11051); in the Quebrada de los Fósiles section, dwarfed forms are present in 8 levels of the 15 analyzed, ranging between 0.3% (MPLP 11073, 5877; BA Pal 6612) and 27.8% (MPLP 11068) (SOI 2).

d) Spores with thickened labra or labra with growths (commonly in the form of verrucae or baculae) (Fig. 6.6, 6.15–6.21). In the Río Seco de la Quebrada section (SOI 2), this group of aberrant spores is present between 0.7% (MPLP 10351) and 7.0% (MPLP 6543) of the total counted specimens. In the Quebrada de los Fósiles section, they are scarcely represented in 6 levels where true fern + Bryophyte spores are recorded, with values from 0.2% (BA Pal 6612, 6613) to 1.7% (MPLP 5877 and 11068).

e) Uneven trilete rays (Fig. 6.5, 6.13–6.14, 6.22–6.23) showing deformed (sinuous) or uneven length of the trilete rays has been observed in one sample in each section: Río Seco de la Quebrada (MPLP 10374, 0.3%) and Quebrada de los Fósiles (BA Pal 6612, 0.2%).

f) Giant forms (Fig. 9.13) are considered significantly larger in size but with identical morphology to known taxa. Lindstrom *et al.* (2019, p. 4, tab. 4) have not mentioned this aberrant size as a teratological trait, but in the QdlF assemblages is quite remarkable. In the Río Seco de la Quebrada section (SOI 2) they were observed between 0.3% (MPLP 10379 and 6543) and 58.0% (MPLP 6544) of the total counting, whereas in the Quebrada de los Fósiles section (SOI 2), on the contrary, they were in 6 of the 17 sampled levels with values of 0.2% (BA Pal 6612, 6613) and 16.0% (MPLP 10366).

g) Unusual presence of fused spores (dyad, triad, tetrad) in the studied assemblages includes *Stereisporites* spp. and *Retusotriletes* spp. (bryophytes, Sphagnales) (MPLP 6543) (Fig. 7.18–7.23), indeterminate spores (Fig. 7.19), and spore clusters referable to *Leschikisporis* spp. (true ferns, Marattiales) (MPLP 11068) (Fig. 7.24–7.26) can indicate difficulties for their dispersion.

Gymnosperm pollen. Pollen grains have variable participation in the palynological assemblages recorded in the QdlF Fm, being rare to common (SOI 1, Fig. 4); they are present in all levels studied in the type section, ranging from 0.3% (MPLP 11068) to 93.5% (MPLP 5877) in the typical section, and in 16 of the 17 studied levels Río Seco de la Quebrada section, 1.3 (MPLP 6544) to 85.4% (MPLP 10348). Abnormal morphotypes of gymnosperm pollen (SOI 2, Fig. 14) are present in 19 of the 22 levels studied the Quebrada de los Fósiles section (range 2.0% to 9.0%) and in 16 of the 17 studied levels Río Seco de la Quebrada section (1.0 to 18.8%).

Only pollen grains with distinctive, abnormal features are considered herein as teratomorphic traits. Monosaccate and bisaccate pollen grains recorded in the QdlF Fm assemblages show variations in the shape and size of the sacs and abnormal thickening in the central body. Following Benca *et al.* (2022, figs. 2 and 4) malformation types in pollen grains we have recognized in the QdlF Fm assemblages:

a) asymmetrical sacci (under-developed or distorted sacci shape), examples see in Figs. 10.8, 10.18, 11.4–11.5, 11.9–11.11, 11.16–11.17, 12.11), and

b) atypical number of sacci (Figs. 10.1, 10.6, 10.9, 10.11, 10.16, 10.18, 10.20–10.21, 11.1–11.8, 11.12–11.15, 11.18–11.20).

We also identified additional differentiable groups:

c) abnormal grain size: giant (Fig. 12.1, 12.3, 12.5–12.7, 12.10, 12.12, 12.15–12.18) and/or dwarf forms (Fig. 12.2, 12.4, 12.8–12.9, 12.11, 12.13–12.14)

d) monosaccate grains with sac malformation showing different aberrations, such as sacs with atypical constrictions of highly variable shape that give a polysaccate appearance (Fig. 10.1–10.8, 10.11–10.15, 10.18–10.20)

Figure 5. Spore tetrads of Sphenophytes/Equisetales (*Calamospora tener*). **1–3,** tetrads with four functional spores (normal forms); **4–7,** tetrads with two functional spores (normal forms) and two non-functional spores (dwarfed form -***df***-); **8–9,** tetrads with three functional spores (normal forms) and one non-functional (dwarfed form -***df***-); **10–13, 29,** incomplete tetrads showing one functional spore (normal form) and two non-functional spores (dwarfed forms -***df***-); **14–17,** functional spore dyads (normal forms); **18–19,** non-functional spore tetrads (dwarfed forms); **20–25,** non-functional spore dyads (dwarfed forms); **26–28,** dyads with one functional spore (normal form) and one non-functional spore (dwarfed form). Scale bar equals 10 µm. For sample number and England Finder coordinates, see SOI 3.

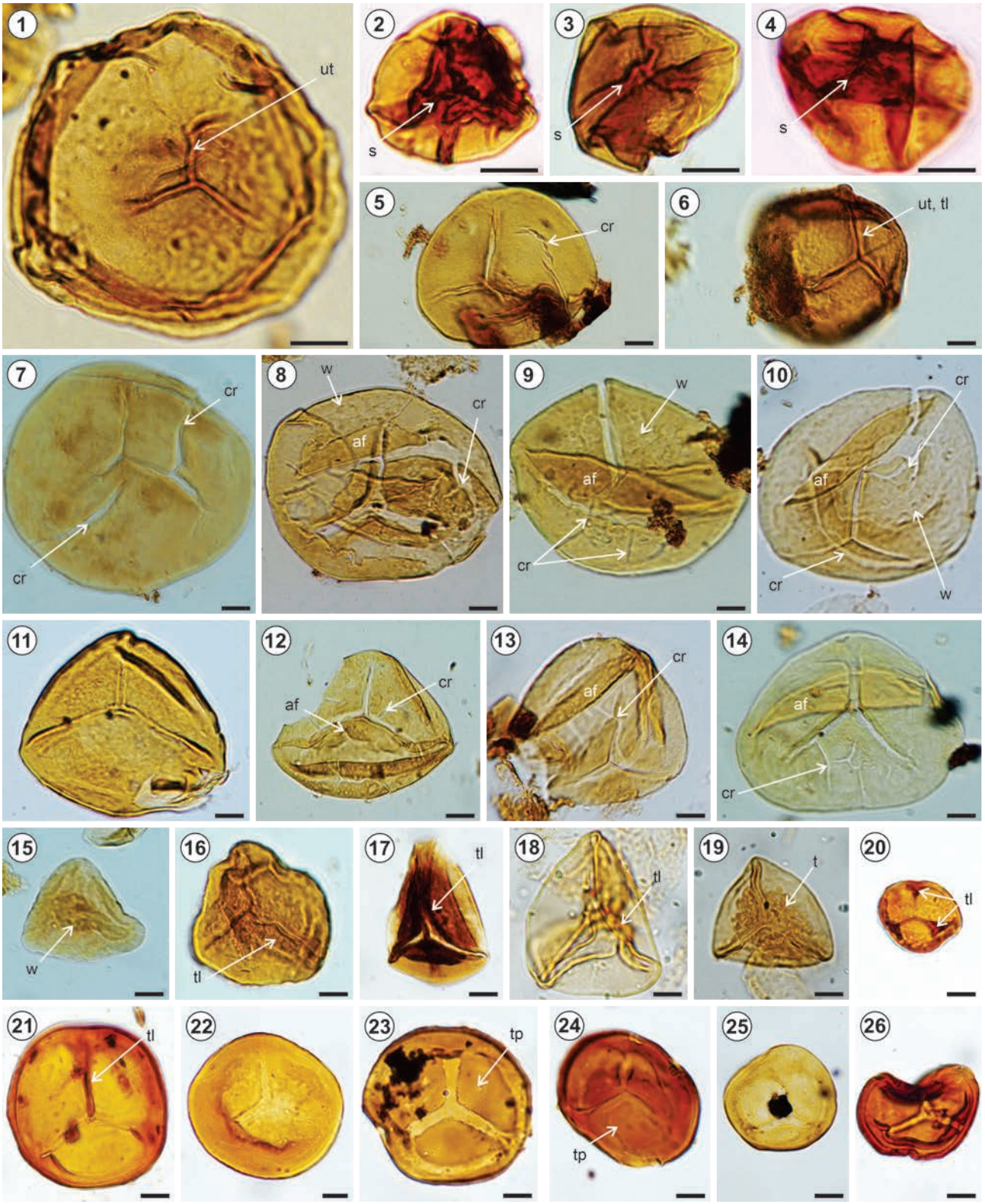

Figure 6. Selected photos of spore's teratology. **1–4,** *Calamospora tener*; **1,** normal form with uneven trilete rays (***ut***); **2–4,** dwarfed and unexpanded specimens showing aberrant folding and thickened labra and deformed trilete mark rays (distinctly sinuous; ***s***). **5–10,** *Todisporites* spp. showing aberrant folding (***af***) and/or cracking exine (***cr***); growths around trilete mark (flat warts, ***w***). **11–14,** *Deltoidospora* spp. showing aberrant folding (***af***) and/or aberrant exine cracks (***cr***). **15–19,** spores referred to *Dictyophyllidites* spp. and *Deltoidospora* spp. with deformed thickened labra -***tl***- and deformed outline (**15–18**) or labra with aberrant growths (**15,** verrucae -***v***-; **19,** baculae -***b***-). **20–26,** spores referred to *Retusotriletes hercynicus* which includes dwarfed forms (**20, 25–26**) compared with normal (**21–22**) forms with thickenings on the proximal face -***tp***-(**23–24**), and with thickened labra (***tl***). Scale bar equals 10 µm. For sample number and England Finder coordinates, see SOI 3.

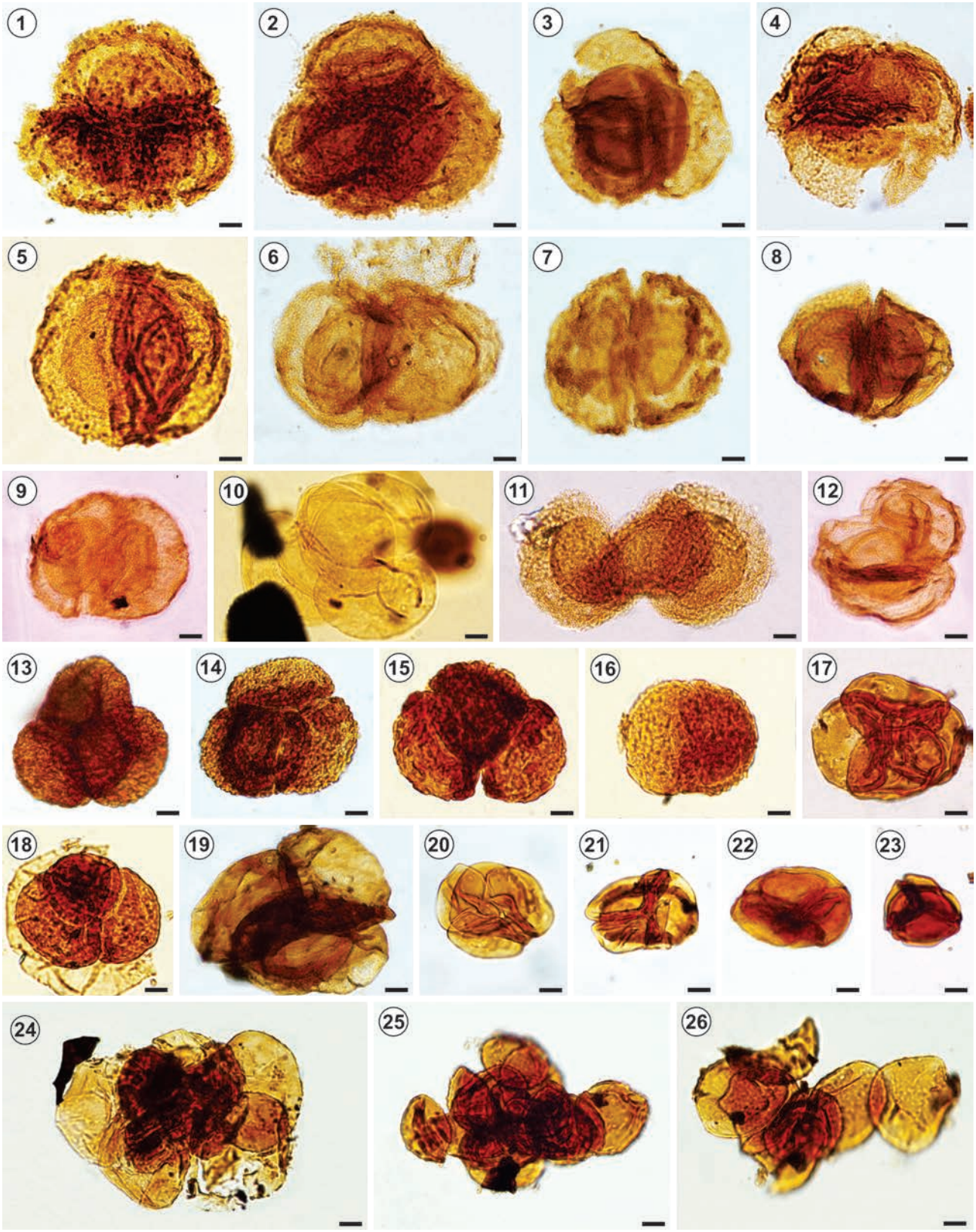

Figure 7. 1–16, 18, Spore tetrads and dyads (see Fig. 14); **1–12,** *Aratrisporites* spp. (Lycophyta-Isoetales); **13–16, 18,** *Secarisporites* spp. (Lycophyta-Selaginellales); **17,** Tetrads of *Carnisporites* spp. (Lycophyta-Selaginellales); **19,** indeterminate spores; **20–23,** *Stereisporites* spp. (Bryophyte, Sphagnales); **24–26,** Spore clusters referable to *Leschikisporis* spp. (true ferns, Marattiales). Scale bar equals 10 µm. For sample number and England Finder coordinates, see SOI 3.

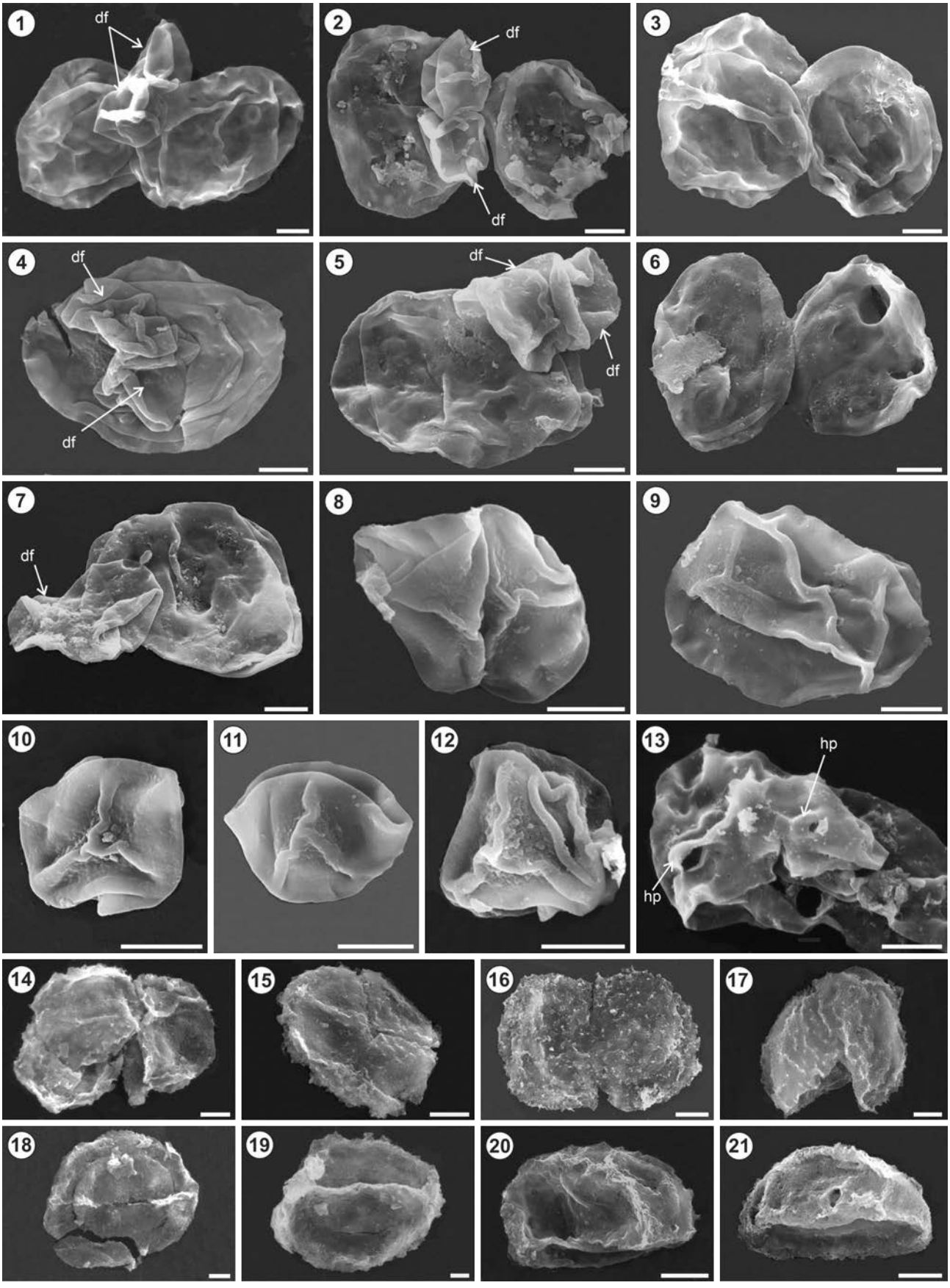
1
df
2
df
df
3
4
df
df
5
df
df
6
7
df
8
9
10
11
12
13
hp
hp
14
15
16
17
18
19
20
21

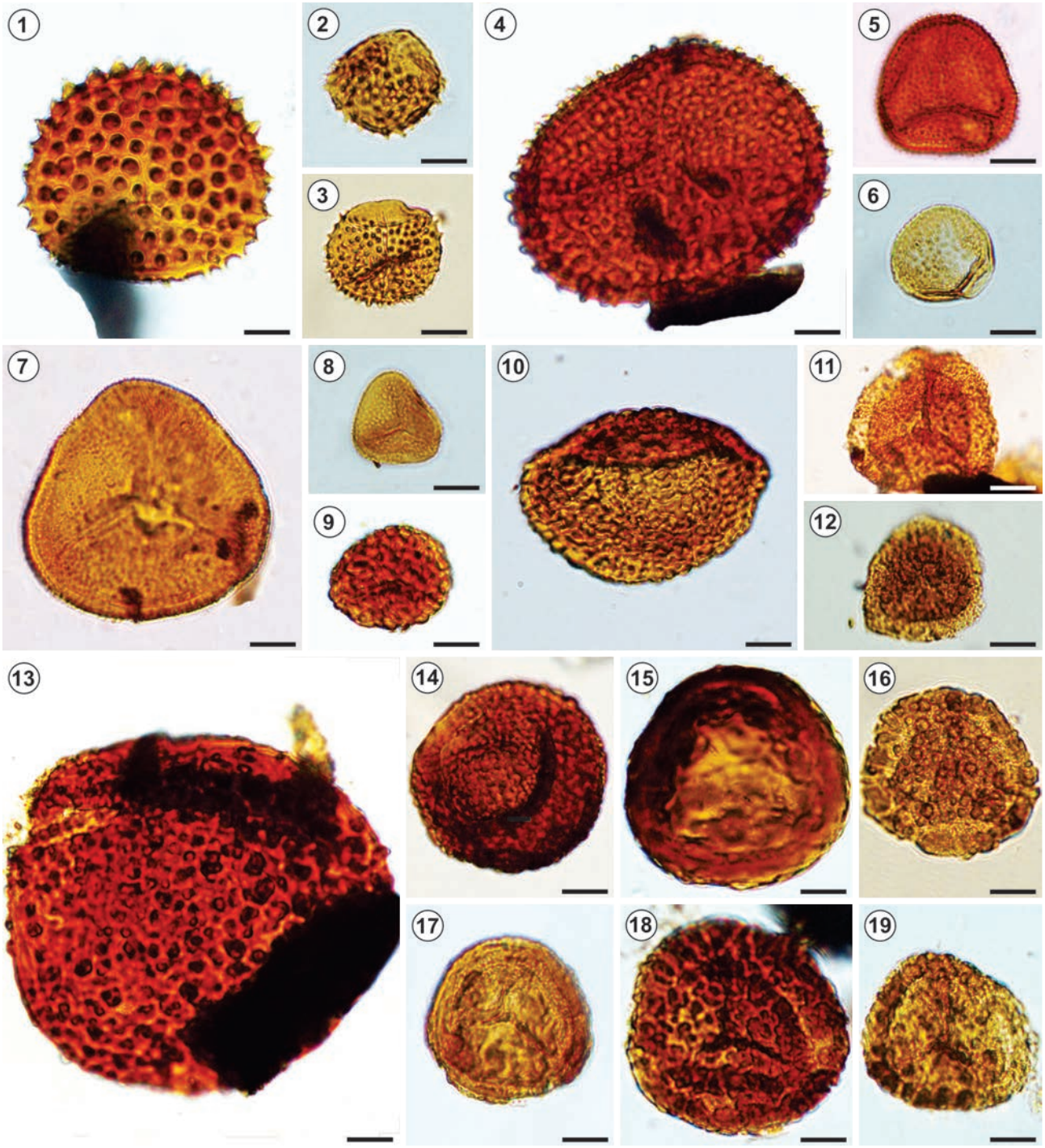

Figure 9. Specimens showing dwarfism in lycopsid and true fern spores: normal sized spores (**1, 4–5, 7, 10–11, 13, 15, 18**) and dwarfed forms (**2–3, 6, 8–9, 12, 14, 16–17, 19**); **1–2,** *Anapiculatisporites* spp. **3–6,** *Brevitriletes* spp. **7–8,** *Lophotriletes* spp. **9–10,** *Rugulatisporites* spp. **11–12,** *Densoisporites* spp. **13–14,** *Verrucosisporites* spp. **15–19,** *Secarisporites* spp. Scale bar equals 10 µm. For sample number and England Finder coordinates, see SOI 3.

Figure 8. 1–12, *Calamospora tener;* **1–2,** Tetrads with two non-functional spores (dwarfed forms -***df***-); **3,** triads with functional spores (normal forms); **4–5,** triads with two non-functional spores (dwarfed forms -***df***-); **6,** dyads with functional spore (normal forms); **7,** dyads with one functional spore (normal forms) and one non-functional spores (dwarfed forms -***df***-); **8,** non-functional spore (dwarfed forms) dyad. **9,** isolated functional spore (normal forms); **10–12,** isolated non-functional spore (dwarfed forms). **13,** Cuticle with small hollow papillae (***hp***). **14–15,** Tetrads of *Aratrisporites* spp.. **16–17,** Dyads of *Aratrisporites* spp.. **18–21,** *Aratrisporites* spp. isolated spores. Scale bar equals 10 µm. For sample number and England Finder coordinates, see SOI 3.

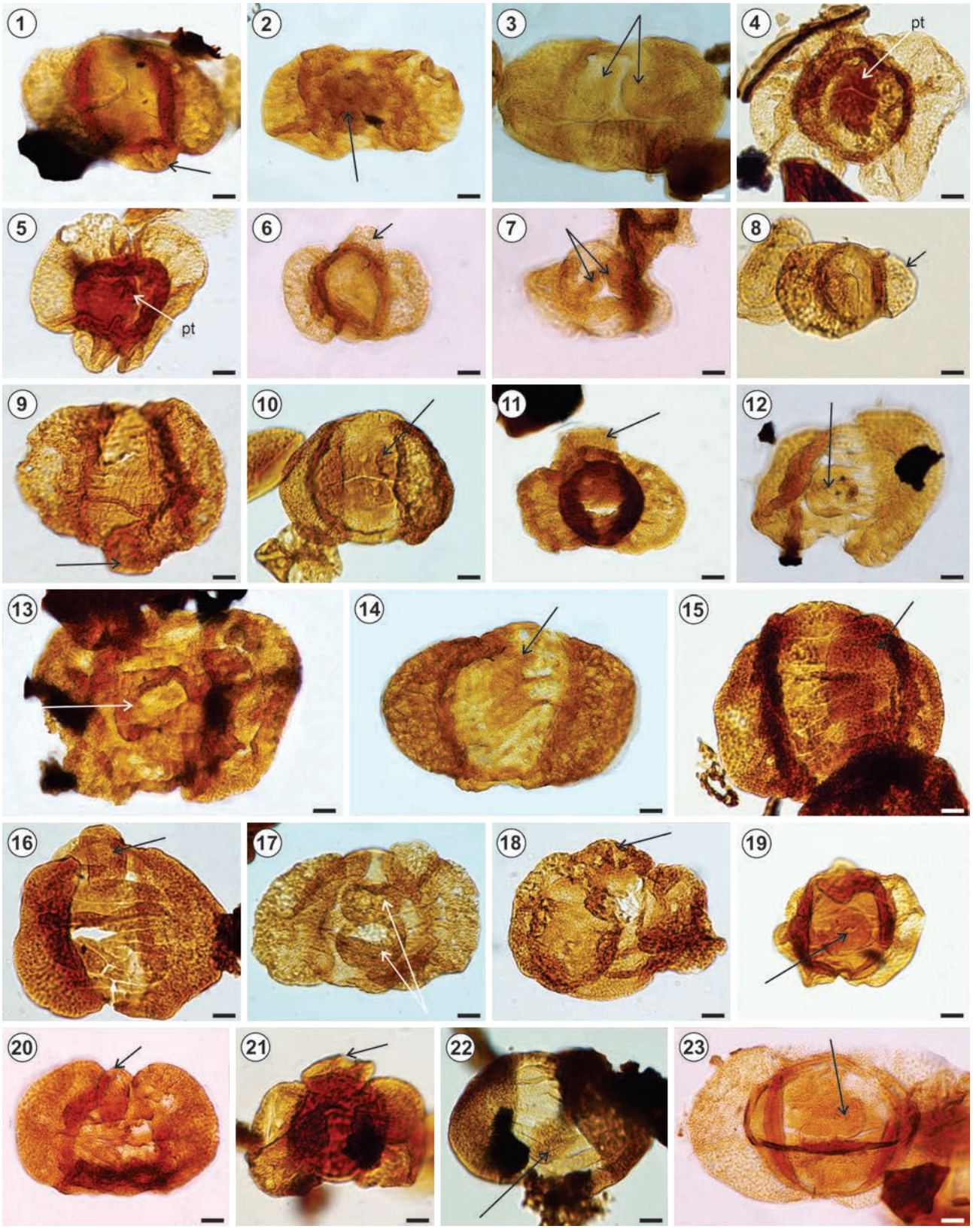
1
2
3
4
pt
5
pt
6
7
8
9
10
11
12
13
14
15
16
17
18
19
20
21
22
23

e) pollen grains with modified thickening of the exines of the central body (Figs. 10.2, 10.4–10.5, 10.7, 10.10)

f) grains showing the central body with irregular exinal protuberances (protosac?) (Fig. 10.1–10.3, 10.9, 10.12–11.23)

g) morphological modifications of taeniae in bisaccate pollen grains (Fig. 10.9, 10.11–10.23) although in very low proportions.

The gymnosperm pollen grains of the QdlF Fm palynoflora (SOI 2, Fig. 14) show malformations in 16 samples from the Río Seco de la Quebrada section, with values ranging from 1.0% (MPLP 11051) to 18.8% (MPLP 10374), represented by: grains with asymmetric sacci, grains with sacci malformations and giant grains. In the Quebrada de los Fósiles section, malformed grains appear in 19 of the 22 samples ranging 2.0% (MPLP 9077, 11064) and 9.0% (MPLP 11073), mainly grains with asymmetrical sacci and pollen with sacci malformations. The following types were identified:

a) Grains with asymmetric sacci, are present in all 15 levels studied in the Río Seco de la Quebrada section (SOI 2), ranging from 1.0% (MPLP 11051) to 11.7% (MPLP 10374); in the Quebrada de los Fósiles section (SOI 2), they are observed in 9 of the 19 levels, with values ranging from 0.8% (BA Pal 6613) to 8.0% (MPLP 11073).

b) Grains with an atypical number of sacci (SOI 2), are observed just in the Río Seco de la Quebrada section in low percentages (0.2–1.2%) in 11 of 15 studied samples.

c) Monosaccate pollen grains with sacci malformations (SOI 2): Río Seco de la Quebrada section in 11 of 15 studied samples, ranging between 0.3% (MPLP 10377) and 3.8% (MPLP 10379); in the Quebrada de los Fósiles section they are observed in 9 samples between 0.3% (MPLP 9085, 10362) and 3.5% (BA Pal 6614).

d) Giant grains (SOI 2) occur in 13 of the 15 samples of the Río Seco de la Quebrada section, between 0.3% (MPLP 10352, 10375, 11052) and 5.5% (MPLP 11056); they are in low proportions in 6 samples of the Quebrada de los Fósiles section 0.2% (MPLP 11072) to 1.7% (MPLP 10362).

e) Dwarf grains (SOI 2), are in 12 of the 15 levels studied in the Río Seco de la Quebrada section, with values ranging between 0.3% (MPLP 11054, 10377, 1374) and 2.0% (MPLP 11056); while in the type locality section, they are in lower percentages 0.2% (MPLP 9085, 10362, BA Pal 6612) to 2.0% (MPLP 9077) in 6 of the studied samples.

f) Grains with a modified thickness of central body and protosaccus (SOI 2), are observed in low proportions in two simples of the type section (MPLP 10362, 0.2%; MPLP, 0.3%), and also, they are observed also in low percentages (0.2% to 0.5%) in eight samples of the 15 studied in the Río Seco de la Quebrada section.

Chlorophytic algae. The ephemeral lacustrine systems and small water bodies developed in the type section of the QdlF Fm, as well as in the Quebrada del Río Seco section, are evidenced by a low, although persistent proportion of algal zygospores (ranging from 0.3% to 98.6% of the total assemblages in Quebrada de los Fósiles section; and 1.1% to 66.5% in Río Seco de la Quebrada (SOI 1, Fig. 4). Within the microphytoplankton, single-celled zygospores of *Ovoidites* are the dominant form within the green algae recorded in both sections studied (Zavattieri *et al*., 2020; SOI 1).

Aberrancies in *Ovoidites* zygospores (Fig. 13.1–13.8) were observed in both studied sections (SOI 2, Fig. 14): in Quebrada de los Fósiles section ranging from 2.5% (MPLP 11072) to 15.3% (MPLP 9076), and Río Seco de la Quebrada section: 0.8% (MPLP 11055) and 2.5% (MPLP 6544).

Figure 10. Aberrancies in bisaccate pollen grains; **1–3,** aberrant grains referred to *Angustisulcites klausii* showing (arrow) a third small protosacs (**1**), protuberance on the central body (**2**) and modified thickness of exine in the central body (**3**); **4–5,** specimens of *Parillinites electus* (4) and *Platysccus* sp. (**5**) showing unusual thickenings (protuberance?, ***pt***) on the central body; **6,** specimen of *Triadispora crassa* showing third small saccus (arrow). **7,** pollen grain referred to *T.* sp. showing thickenings in the exine of the central body (arrows); **8,** indeterminate saccate pollen showing sacs of asymmetrical sizes, with one saccus smaller than the other (arrow); **9,** specimen of *Hamiapollenites* sp. showing a small aberrant saccus and distorted taeniae (arrows); **10,** *Lunatisporites* sp. showing exinal thickening on the central area of the central body (arrow); **11–12,** *Striatopodocarpites* spp. showing a small sac (arrow) (**11**) and thickenings (protuberances) on the central body (**12**); **13, 22,** specimens of *Protohaploxypinus amplus* showing thickenings (protuberances) on the central body that distort the taeniae (arrows); **14–15,** specimens of *Protohaploxypinus* spp. showing exinal thickenings on the proximal (**14**) and distal (**15**) faces of the central body, resembling a protosaccus (arrows); on the proximal face they distort taeniae; **16, 18–19, 21,** pollen grains of *Striatoabieites* spp. showing protuberances of various shapes on the central body (arrows) (**16, 19**), protosaccus (**16, 18**), lobed saccus (**19**) and a third saccus (**21**); **17, 20**, Indeterminate saccate pollen showing protosaccus on the distal face (**17**) and on lateral margin of the grain (**20**); **23,** specimen of *Striatopodocarpites pantii* showing exinal thickening on the central body (arrow). Scale bar equals 10 µm. For sample number and England Finder coordinates, see SOI 3.

DISCUSSIONS

Palynomorph teratology interpretations

The teratology reflects different types of disturbance during spore and pollen formation, which may indicate various forms of environmental stress. Lindström *et al.* (2019) used fern spore teratology spikes as a proxy for ecological stress and possible mutagenesis in land plants across the Triassic–Jurassic boundary (TJB) in northern European basins, correlating the teratology record with the Central Atlantic Magmatic Province (CAMP) volcanism and as evidence for the emissions of toxic volcanogenic substances (mainly environmental mercury spikes). They examined the teratology of smooth-walled trilete fern spores in five categories, describing malformations. They categorized the teratology in five-step severity scale and possible causes of such disturbance during different developmental stages (Lindström *et al.,* 2019, fig. 2, tab. 1).

Spores of Equisetales. The Equisetales produce *Calamospora* spores. This morphogenus is one of the dominant groups recorded in the QdlF Fm palynological assemblages (*ca.* 25.1% in the Río Seco de la Quebrada section; *ca.* 7.7% in Quebrada de los Fósiles section; SOI 1). Phenotypically normal fused spores of *Calamospora* (tetrads, triads, dyads) are abundant in the studied palynological assemblages. However, other malformed ones that have at least one aberrant spore (dwarfed, unexpanded, folding, with labra thickened/ with growths and/or with deformed outline forms) are also frequent. These aberrant spores are commonly found dispersed in studied microscopic slides (Figs. 5, 8). Thus, in the present context, we consider that most malformed spores (fused and dispersed) may reflect reactions to adverse environmental conditions.

Dispersed tetrads of the sphenophyte *Calamospora* showing aborted spores and size variation may indicate disturbance and unbalanced or incomplete cell division (incomplete or unbalanced cytokinesis), including non-functional spores in the tetrads. Extant and Mesozoic Equisetales are typical hygro-hydrophytic vegetation, and frequently they grow marginally to the rivers, on levees, and wet soils surrounding water bodies in the floodplain. However, these horsetails were also likely colonizers of disturbed habitats (Kelber & van Konijnenburg-van Cittert, 1998; Ruffo Rey, 2021).

Spores of Lycophytes. The frequent to common occurrence of spore tetrads in Lycophytes is also a possible indication of harmful environmental stress (Visscher *et al.*, 2004; Looy *et al.*, 2005). Ram-Awatar (2011) also pointed out that large amounts of unseparated spore tetrads in fossil lycophyte assemblages could be an environmental stress response.

The individual microspore tetrads of herbaceous lycopod (Pleuromeiales) producers of *Aratrisporites* appear to be morphologically mature when they possess well-developed ornamentation and known range size (Saxena *et al.*, 2015; Chu *et al.*, 2021). Saxena *et al.* (2015) recorded unusual *Aratrisporites* tetrads and they deduced that unfavorable climate conditions might have induced changes in the plant physiological processes (*e.g.*, non-functional tapetum, altered pH values in the microsporangium or the inactive callase organic compound) that prevented the dissociation of tetrads into individual spores. Normal sporogenesis needs specific pH values inside microsporangium, the release of callase enzyme, the disintegration of the callose walls, and the ultimate release of the single spore from the tetrads. Thus, Saxena *et al.* (2015) deduced that extreme climatic conditions might have triggered some malfunctioning in the sporogenesis process that altered the specific pH values inside the microsporangium, and its consequent mentioned alterations.

As mentioned in the result section, fused specimens (dyads, triads, tetrads and clusters, Figs. 7.1–7.17, and Figs. 8.14–8.17) of Lycophyte are common components in some levels of the QdlF Fm assemblages (Fig. 14; SOI 2) and their presence do not necessarily represent a product of disturbed environments. Malformed tetrads of the lycopsid microspores are also recorded in the QdlF Fm, indicating disturbance affecting cell growth and/or unbalanced cytokinesis (Lindström *et al.*, 2019). Nowak *et al.* (2019) considered that aberrant tetrads are associated with teratological spore-pollen, may indicate an alteration in the reproductive capacity of the producing plants, and can be interpreted as adaptations to extreme conditions.

Spores of true ferns and Bryophytes. The low frequencies of hydro-hygrophyte trilete laevigate spores produced by fern families and bryophytes recorded in both sections of the QdlF Fm (SOI 1, Fig. 4) suggest that this riparian vegetation grew in unstable environmental conditions, like dry sites and/or withstanding periods of drought (Taylor *et al.,* 2009). Some circular to triangular bryophyte and true fern

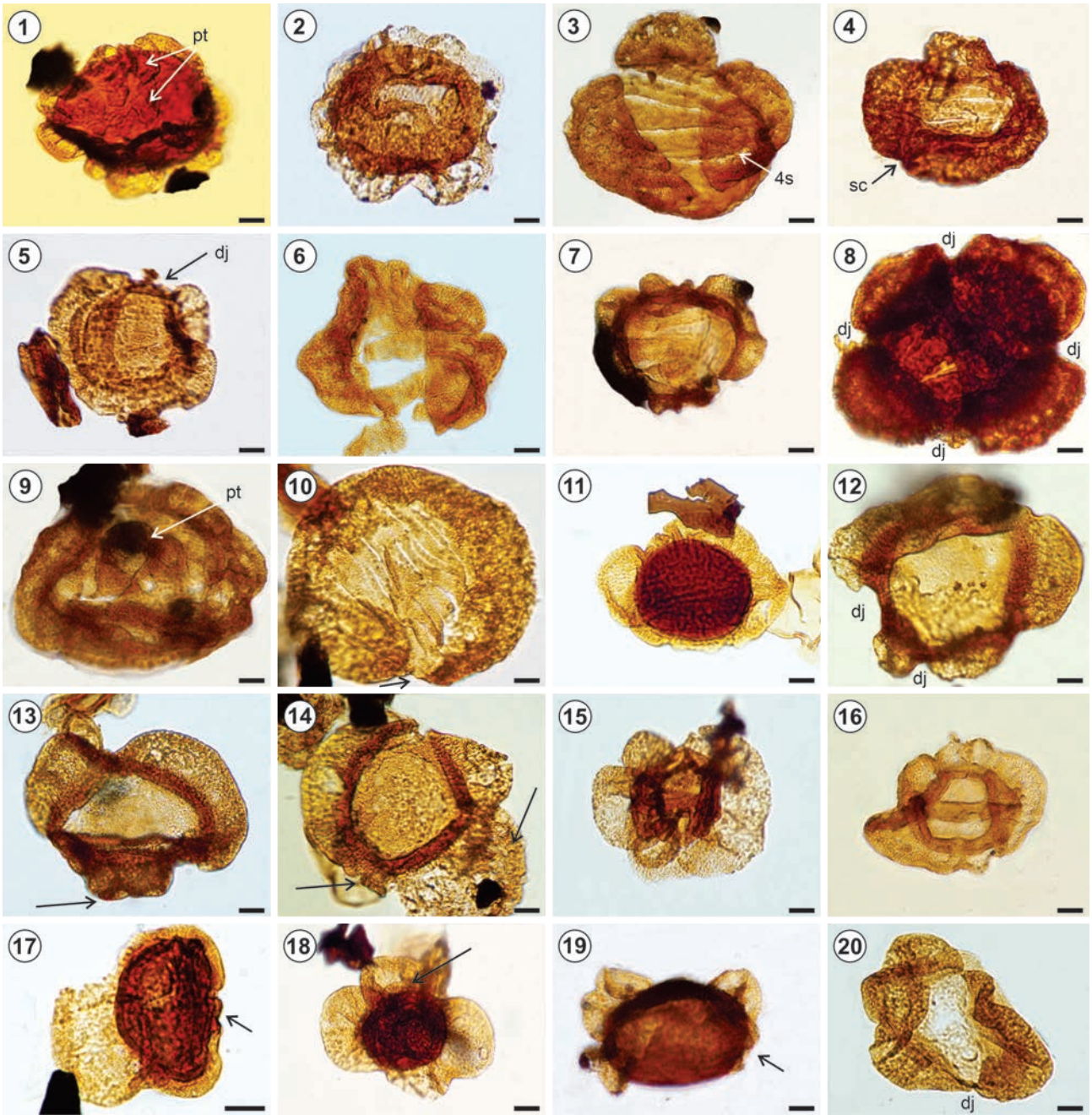

Figure 11. Aberrancies in monosaccate pollen grains; **1–2,** Pollen grains referred to *Bascanisporites undosus*. Specimen with lobed saccus (***ls***) resembling a polysaccate state; also (**1**) small protuberances/pseudosacii (***pt***) can be seen on the central body of the grain; **3,** trisaccate pollen grain (*Crustaesporites globosus*) with an exinal growth (exoexine) on the lower right part of the central body resembling a fourth sac (***4s***); **4–9**, pollen grains referred to *Goubinispora morondavensis*: specimens with markedly lobed sacs, irregularly shaped, from slight constrictions (***sc***); (**4, 9**) to marked sac disjuncture (***dj***) (**5, 8**), resembling polysaccate grains; conspicuous protuberances (***pt***) on the central body are observed in some specimens (**9**); **10,** specimen of *Striomonosaccites ovatus* exhibiting a marked discontinuous sac (arrow), associated with a deformation in the central body; **11,** indeterminate monosaccate pollen grain of bilateral symmetry with marked and irregular constrictions; **12,** specimen of *Variapollenites rhombicus* showing deformations and marked discontinuous sac (***dj***); **13–14,** specimens of *V. trisulcus* exhibiting malformations of sacs (arrow); **15–16,** specimens of *V.* spp. with strong lobulated sacs in variable forms giving a polysaccate aspect (**15**) to variably lobulate monosaccate (**16**); **17–20,** aberrant un-determinate pollen grains exhibiting strong deformations (arrow), from undeveloped sacs (**17, 19**), to overlapping sacs (**18**) and a sac with constrictions and discontinuous sac resembling lobated monosaccate to polysaccate grains. Scale bar equals 10 µm. For sample number and England Finder coordinates, see SOI 3.

spores show abnormal features in their morphology, regarded here as aberrant forms. Dwarfed and unexpanded forms recorded in these assemblages, would suggest "minor teratological severity" caused by premature shedding from the sporangia, according to interpretations given by Lindström *et al.* 2019 (fig. 2, tab. 1). Meanwhile, uneven trilete rays, aberrant folding (exines with transverse folds), and/or cracking of the exine, as well as thickened labra or labra with deformations (*e.g.*, growths, commonly in the form of verrucae or baculae) would reflect "minor to moderate teratological severity", possibly caused by mild genetic disturbance (cf. Lindström *et al.,* 2019, p. 4, tab. 1).

As indicated in the Results section, tetrads and spore clusters of bryophytes and true ferns are observed in the studied associations. Visscher *et al.* (2004) interpreted unseparated spore tetrads in Permian–Triassic lycophytes as unusual mutated palynomorphs based on the UV-B radiation effects caused by the release of huge amounts of organo-halogen gases into the atmosphere caused by extensive volcanic eruptions of the large Siberian area. Looy *et al.* (2005) linked the enormous production of tetrads during the Triassic period to environmental changes that affected the regular sporogenesis cycle in some specific taxonomic groups. However, these unseparated spore tetrads could not a signal of global mutagenesis, and probably more likely they were an adaptative response to

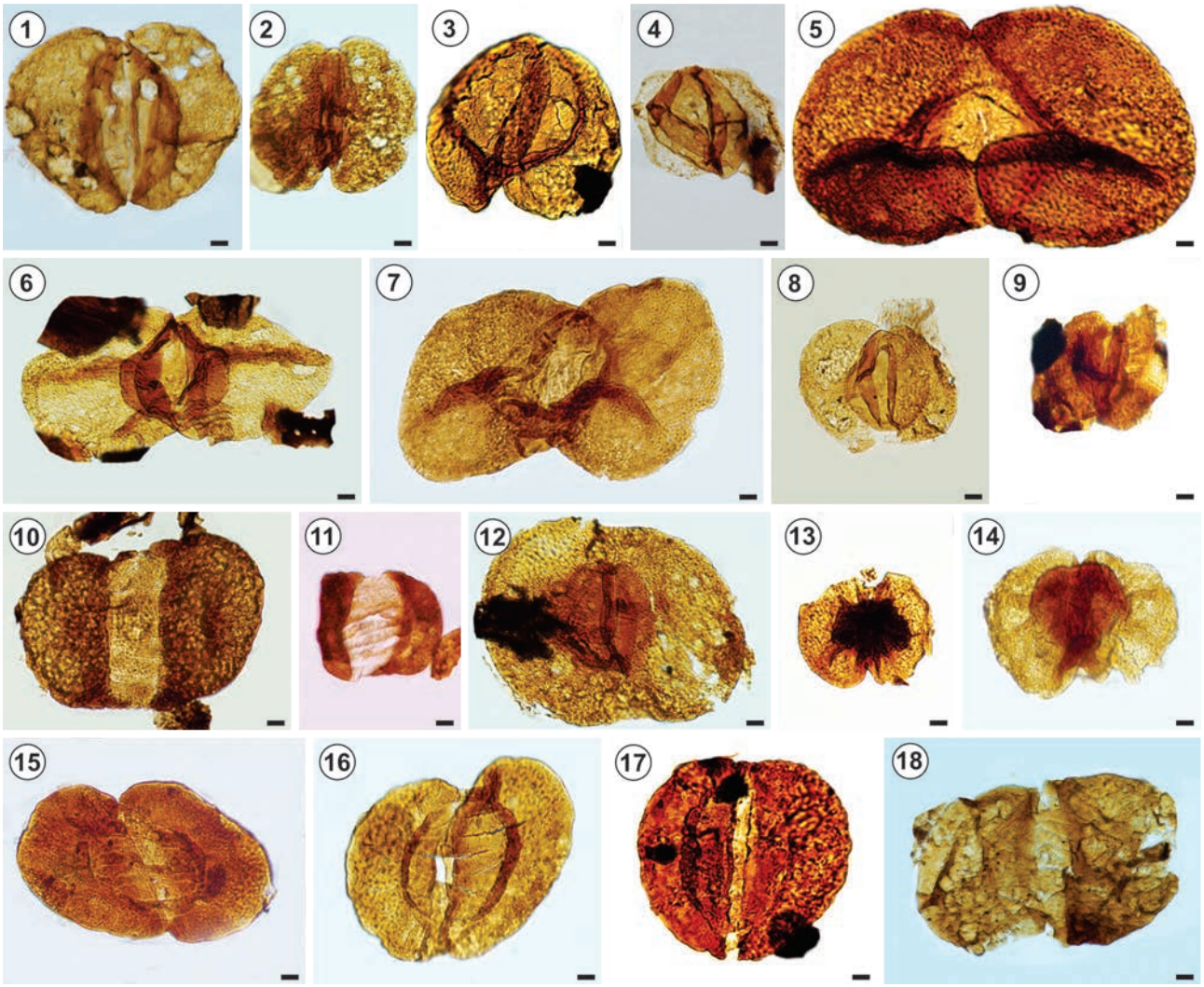

Figure 12. 1–4, 6–14, Examples of gigantism in saccate pollen grains compared to normal forms; *Alisporites cymbatus*; **3–4,** *Alisporites* sp. cf. *A. asansoliensis*; **6–9,** *Platysaccus plicatus*; **10–11,** *Protohaploxypinus amplus;* **12–14,** *Rhizomaspora indica;* **5, 15–18,** Examples of gigantism (overgrowth) in pollen grains: **5,** *Angustisulcites grandis,* **15,** *Striatopodocarpites balmei,* **16,** *S. oblongatus,* **17,** *Protohaploxypinus goraiensis,* **18,** *P. sewardi.* Scale bar, 10 µm. For sample number and England Finder coordinates, see SOI 3.

environmental stress, because is found no developmental deviations in spore shape or the wall ultrastructure, and discovered that the spores within these tetrads were fully mature. Furthermore, these mature spores within the unseparated tetrads were never fused together but rather loosely linked to each other interlocking elements of the paraexospore at either interradial contact area or equatorial region. According to Lindström *et al.* (2019, tab. 1), these mutagenetic features affecting cell growth indicate disturbed meiosis (resulting in either a tetragonal tetrad configuration, or more than four spores, or due to fused twins), unbalanced and incomplete cytokinesis (sporogenesis or cell division), all of which may indicate moderate to severe teratology. Thus, in the present context, we consider most of the tetrads to reflect reactions to adverse environmental conditions. We quantify the numbers of abnormal tetrads in relation to normal forms (expressed in %; see Result section and Fig. 4).

Nowak *et al.* (2019) considered that tetrads associated with teratological spores may indicate an alteration in the reproductive capacity of the producing plants and can be interpreted as adaptations to extreme conditions.

Gymnosperm pollen grains. As mentioned above (in the Results section), the main teratology categories observed in the pollen grains include: asymmetrical sacci, atypical number of sacci, different sizes (dwarf and/or giant forms), or modified thickness of exines of the central body, or surface anormal features. The present material also includes morphological modifications of taeniae in bisaccate pollen grains. Monosaccate pollen grains recorded in the QdlF Fm assemblages also show variations in the shape and size of the sacs (*i.e.*, with atypical constrictions of highly variable shapes that give a polysaccate appearance).

Foster and Afonin (2005) pointed out that malformations in saccate pollen around the Permian–Triassic boundary was the result of deteriorating atmospheric conditions. Studies of both extant and fossil plants suggest that normal sporogenesis results in 95 to 97% normal viable spores and 3 to 5% are abnormal grains (Foster & Afonin, 2005; Saxena *et al.*, 2015; Lindström *et al.,* 2017, 2019; Benca *et al.*, 2022). Previous studies of fossil and modern gymnosperm pollen suggested that >3% of malformed grains are associated with environmental stress (Foster & Afonin, 2005; Hochuli *et al.*, 2017; Fijałkowska-Mader, 2020; Benca *et al.*, 2022). Thus, phytotoxicity and environmental stress is evidenced by a benchmark of >3% malformations in the dispersed fossil record (Rabe & Haufler, 1992; Mičieta & Murín, 1996; Lindström *et al.*, 1997; Foster & Afonin, 2005). Benca *et al.* (2018, 2022) demonstrated that heightened malformed pollen frequencies can indicate enhanced ultraviolet-B (UV-B) radiation exposure and associated radiative stress by ozone-depletion caused by Siberian Traps magmatism which provoked the end–Permian crisis. Such remarkably environmental crises influenced the reproductive biology of Permian–Triassic conifers, peltasperms, corystosperm seed ferns, and potentially other conifers that were affected by intense ionizing and ultraviolet (UV–B) radiation due to a stratospheric ozone collapse caused by volcanic emissions (*e.g.*, Dzyuba, 1998; Ries *et al.*, 2000; Visscher *et al.*, 2004; Foster & Afonin, 2005; Koti *et al.*, 2005, 2007; Beerling, 2007; Lomax *et al.*, 2008). Restricted stratigraphic intervals with more abundant abnormal pollen (Fig. 14, SOI 2) may indicate temporal volcanic events and consequent periods of increased atmospheric pollution and the affectation of the environment of the QdlF Fm.

Chlorophytic algae. The dominance of zygospores or possibly aplanospores of green algae recorded in both studied sections suggests that water bodies of the floodplains (shallow lakes, streams, swamps, or ponds) were not deep (absence of thick organic pelites) and may have dried out periodically due to seasonal warming. Desiccation of their habitat, probably have been subjected to seasonal aridity (see Zavattieri *et al.*, 2020). Massive occurrences of *Ovoidites* interpreted as blooms of zygnematacean algae may reflect successions of seasonal events or a low contribution of the water courses to the sites of deposition (scarce supply of water). Aberrancies in *Ovoidites* zygospores could also suggest physical and/or chemical changes in the water bodies and might have provoked environmental hazards on the zygnematalean populations. Environmental stresses, such as salinity, aridity, and ashes caused by volcanism, are considered here as main causes that created unstable conditions in water bodies. Fine and densely distributed root casts indicate the development of incipient paleosols and also suggest that the water bodies might be periodically dried out, subjected to intermittent aridity.

Plant tissues. Evidence of developmental deviations

Palynological samples of the studied levels of the QdlF Fm from both sections contain dispersed, and well-preserved fragmentary cuticle remains. The cuticle is a thin extracellular layer that overlies the epidermis and protects the plant against drought and moisture stress (Kerp, 1990). It is difficult to determine the botanical affinities of these cuticle fragments as they lack distinctive macromorphological features. The presence of well-preserved hairs and trichomes would indicate little transport (Figs. 8.13, 13.9–13.24). Cariglino *et al.* (2018) recorded and described *Ptilozamites* cuticles from the AMZ1 level in the type section of the unit (Fig. 2.1). These plant debris are characterized by thick cuticles with sunken stomata, trichomes, and papillae, which are interpreted to represent xeromorphic adaptations to reduce the water loss (Kerp, 1990), and may be related to adverse microenvironmental conditions created by volcanic episodes that occurred during the deposition of this unit. Abnormal growth features on plant cuticles or epidermal cell shape can result from environmental stress due to sudden changes related to weather (*e.g.*, drought, waterlogging, temperature changes), in which case the environmental stress could be seasonal (Martínez *et al.*, 2020; Pott *et al.*, 2008). Mentioned epidermal cell division deviations might be tied to the repeatedly explosive volcanism generating regional stratospheric ozone holes (Kutterolf *et al.*, 2013; Black *et al.*, 2014). Increased levels of ultraviolet-B (UV-B) radiation associated with ozone-layer depletion have been invoked as a possible mutating agent (*e.g.*, Archangelsky *et al.*, 1995; Visscher *et al.*, 2004; Del Fueyo *et al.*, 2013). Pulsed volcanism could well account for periods of time of various stresses the plants would need to endure while actively growing. Phytotoxic substances can induce stress responses and cause morphologically visible abnormalities in their cuticles.

Paleoenvironmental and paleoclimatic considerations. Volcanism and its environmental effects on paleoecosystems

Tectonics, volcanism, and climate are directly and indirectly related (Spalletti *et al.*, 2003). In the western margin of southern South America, episodes of extensional rifting coincident with the intense magmatism of the Choiyoi Magmatic Province occurred between the early Permian and early Triassic as well as during the Middle to Late Triassic when the Puesto Viejo Group was deposited (post-Choiyoi Magmatism, Sato *et al.*, 2015). Extensional rifting episodes and consequent intense explosive volcanic activity occurred in the San Rafael region during the Middle Triassic, which conditioned the composition and disposition of the sedimentary strata and volcanic (basalt and ignimbrites) rocks of the QdlF Fm (Monti & Franzese, 2016, 2019). The volcanic events that occurred during the deposition of the QdlF Fm are evidenced by abundant rhyolitic air fall tuffs that are preserved and/or integrated to deposits within the floodplain. Tabular pyroclastic flows would have been formed from the collapse of eruptive columns associated with nearby explosive volcanic activity (Cariglino *et al.*, 2018). Monti and Franzese (2016) interpreted that acid ignimbrite flows that covered fluvial deposits of the QdlF Fm could have generated a hydrological imbalance accompanied by local climate modifications towards more arid conditions. Sub-volcanic basaltic intrusives also affected mainly the fine deposits of the unit, evidenced by the common presence of peperites (observed in the Río Seco de la Quebrada Creek) (Vázquez, 2013; Ottone *et al.*, 2014; Cariglino *et al.*, 2018). Among the phenomena produced by such large explosive volcanism, besides considerable ash effusions, emissions of greenhouse gases, like volcanogenic halogen-bearing (*e.g.*, chlorine and bromine) compounds into the stratosphere changing its chemistry, the acid rain, and ozone layer depletion and consequent changes in the radiation could have caused important impacts in the ecosystem and/or on climate (Kutterolf *et al.*, 2013; Black *et al.*, 2014; Cadoux *et al.*, 2015; and references therein). As mentioned previously by Cariglino *et al.* (2018), even if the strong volcanic activity of the post-Choiyoi magmatism did not occur catastrophically during the Middle Triassic (as has been demonstrated in the large IMP (Ignean Magmatic Province that caused extinction events), but continuous explosive volcanism (even when occurred episodically in short lapses of time) produced changes into the atmosphere, water bodies and soils affecting the biota. Each eruption could induce regional to even global environmental impacts.

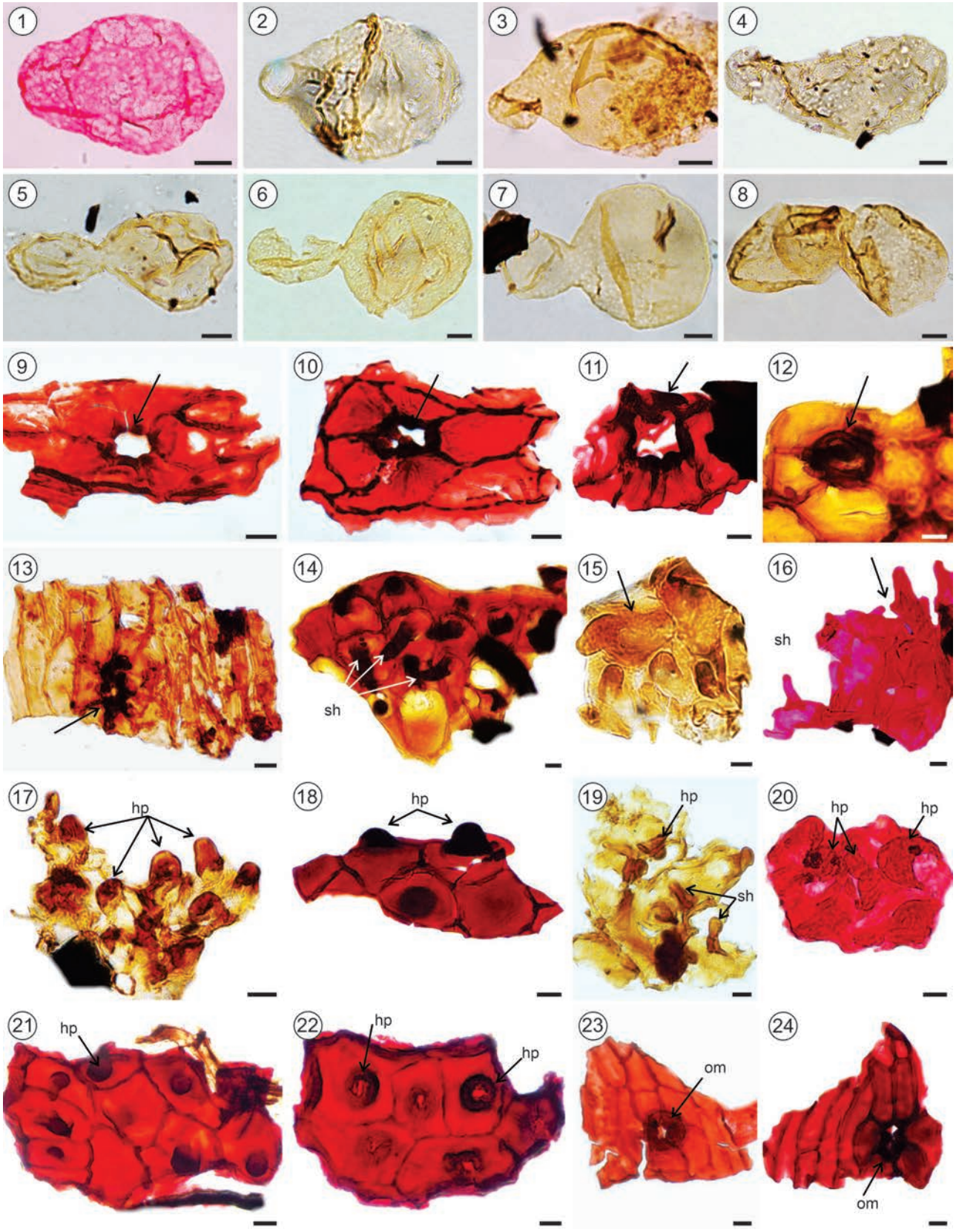

Figure 13. 1–8, Aberrant forms of *Ovoidites* spp. (Zygnematacea); **9–24,** xeromorphic structures in dispersed cuticle fragments; **9–13,** clogged stomata (arrow); **14–19, 21–22,** cells with small hollow papillae (***hp***) and short single-celled hairs (***sh***). **20,** clogged stomata and small hollow papillae; **23–24,** thickening of the ostiole margins (***om***); **24,** clogged stomata. Scale bar equals 10 µm. For sample number and England Finder coordinates, see SOI 3.

Composition of the flora of the Quebrada de los Fósiles Formation and paleoenvironmental significance

The distinctive plant remains and co-occurring palynofloral assemblages of the QdlF Fm, recovered from the type section as well as from the Río Seco de la Quebrada section (Vázquez, 2013; Ottone *et al.*, 2014; Coturel *et al.*, 2016; Cariglino *et al.*, 2018; Zavattieri *et al.*, 2020; Gnaedinger *et al.*, 2020; Gutiérrez & Zavattieri, 2021). The wetland and peculiar floral assemblages recovered from the type section of the unit consist of lycophytes (*Pleuromeia* and *Lepacyclotes*), sphenophytes (*Equisetites* and *Neocalamites*), and seed ferns (*Ptilozamites*) (Cariglino *et al.*, 2018), and remarkably, an equisetalean stem attributed to *Neoarthropitys* and *Nododendron* (Gnaedinger *et al.*, 2020). Most of these plants were possibly stress-tolerators (Looy *et al.*, 2021). Particularly, *Pleuromeia* is a producer of the Permian–Triassic unseparated spore tetrads (Visscher *et al.*, 2004; Looy *et al.*, 2005), and it was likely very slow growing and a poor ecological competitor, only able to persist in places where few other plants could grow (Looy *et al.*, 2021). Sphenophyte remains were also recorded in the tuffaceous carbonaceous pelites and thin coal levels cropping out in the Río Seco de la Quebrada Creek (Fig. 3.5–3.10). The preservation of the macroflora in fine-grained tuffaceous sediments points to volcanic events occurring episodically during the deposition of the unit, causing stressful environmental conditions. Thus, plant communities in this volcanic landscape persisted under abnormal environmental stresses.

The palynofloral assemblages recorded in both studied sections evidence greater diversity than the floral remains (Fig. 4). AMZ1 and GzD section levels report Pleuromeiaceae and equisetalean plant remains (Coturel *et al.*, 2016; Cariglino *et al.*, 2018; Gnaedinger *et al.*, 2020). Thus, the high representations of their dispersed microspores evidence local vegetation. Spores of lycophyte and sphenopsids dominate the studied microflora, whereas pteridophyte and bryophyte (smooth and ornamented trilete spores) show low participation (Fig. 4, SOI 1). Hydrophytic-mesophytic plants inhabited moist lowland environments (swamp, marsh, ponds, and riparian river margins) surrounding the depositional area. *Pleuromeia* was adapted to arid environments in with seasonal to perennial moisture habitats, such as a seasonal dry river or stream channels, ephemeral pools, or other water bodies (Taylor *et al.*, 2009). Sphenopsids are also well-suited to arid environments, where they can locally thrive in river valleys, oases, or possibly marshes and swamps. These spore-bearing plants can require just moist to wet lowland environments surrounding the depositional area. However, they can also colonize drier environments provided they have seepages (infiltrations) and some moisture available in and around the depositional environments (Abbink *et al.*, 2001, 2004; Kustatscher *et al.*, 2012; Paterson *et al.*, 2016, 2017; Lindström *et al.*, 2017; Baranyi *et al.*, 2019; Looy *et al.*, 2021).

Gymnosperm pollen grains are dominated by pteridosperms (peltasperms, caytoniales, and corystosperm seed ferns) and conifers (coniferales and voltziales), while ginkgoaleans and cycadaleans have scarce representation through the sampled succession of both sections (Fig. 4, SO1). The ecosystem from that pollen grains was derived, might have been surrounding areas to the sites of deposition mainly inhabited by conifers, mostly pteridosperms that contributed the scarce allochthonous elements. Gymnosperms are mainly restricted to humid environments and colonize based in water availability (Benca *et al.*, 2018). The low percentages of pollen grains on both studied sections could suggest a selective pressure due to low water availability by environmental stress.

The dominance of zygospores or possibly aplanospores of green algae recorded in aquatic deposits dried out periodically by seasonal aridity. This could support ephemeral or seasonally dry pools in an arid or sub-arid region with mixed communities of lycopsids, sphenopsids, and various seed plant lineages.

The co-occurrence of several morphological aberrancies observed in the morphology (teratogenesis) of spores (Sphenophytes, Lycophytes, true ferns, Bryophytes), pollen of Gymnosperms *s.l.*, and Zygnemataceae zygospores, the genetic disturbance affecting cell growth of tetrads (incomplete cytokinesis) and cuticle remains having modified structures revel concurrent proofs of adaptation of the terrestrial and aquatic vegetation to adverse environmental conditions. Altogether, provide independent evidence of a deteriorating atmosphere caused by extensive volcanic activity and affecting the development of the plant communities within the ecosystem (SOI 2, Fig. 14).

The terrestrial and aquatic vegetation of the QdlF Fm

grew associated with shallow water bodies in floodplain environments developed under warm temperate, strongly seasonal arid to semiarid climate during deposition of the unit —based on the paleogeographic position of Triassic basins of Argentina and the paleoclimatic belts distribution according to Artabe *et al.* (2003) and Spalletti *et al.* (2003). Thus, the macro and microflora reflect sub-environments in which the vegetation was developed rather than seasonal sub-humid climatic conditions as previously inferred (Spalletti, 1994; Kokogián *et al.*, 2001; Tassi *et al.*, 2013; Monti, 2015; Monti & Franzese, 2016 and references therein). Mancuso *et al.* (2021) recently referred to warm temperate seasonal semiarid conditions for the Middle Triassic, mainly based on vertebrate components and their climatic context. Meanwhile, Pedernera *et al.* (2022) inferred that the Middle Triassic paleofloras of Argentina developed under an arid to subhumid climate with precipitation concentration during summers.

CONCLUSIONS

Here we document the first occurrence of synchronous teratologic traits across multiple plant spores and pollen, and possibly chlorophytic algae within the same region coinciding with nearby repeated explosive volcanism causing developmental disturbances throughout entire plant communities in the geological past. The malformed palynomorphs and possibly cuticles in this study could have all directly resulted from this phenomenon in combination with other stresses volcanic eruptions provoke.

Middle Triassic flora (plant and palynoflora assemblages) of the Puesto Viejo Group, San Rafael Depocenter (Mendoza Province, Argentina), have been recorded, up to

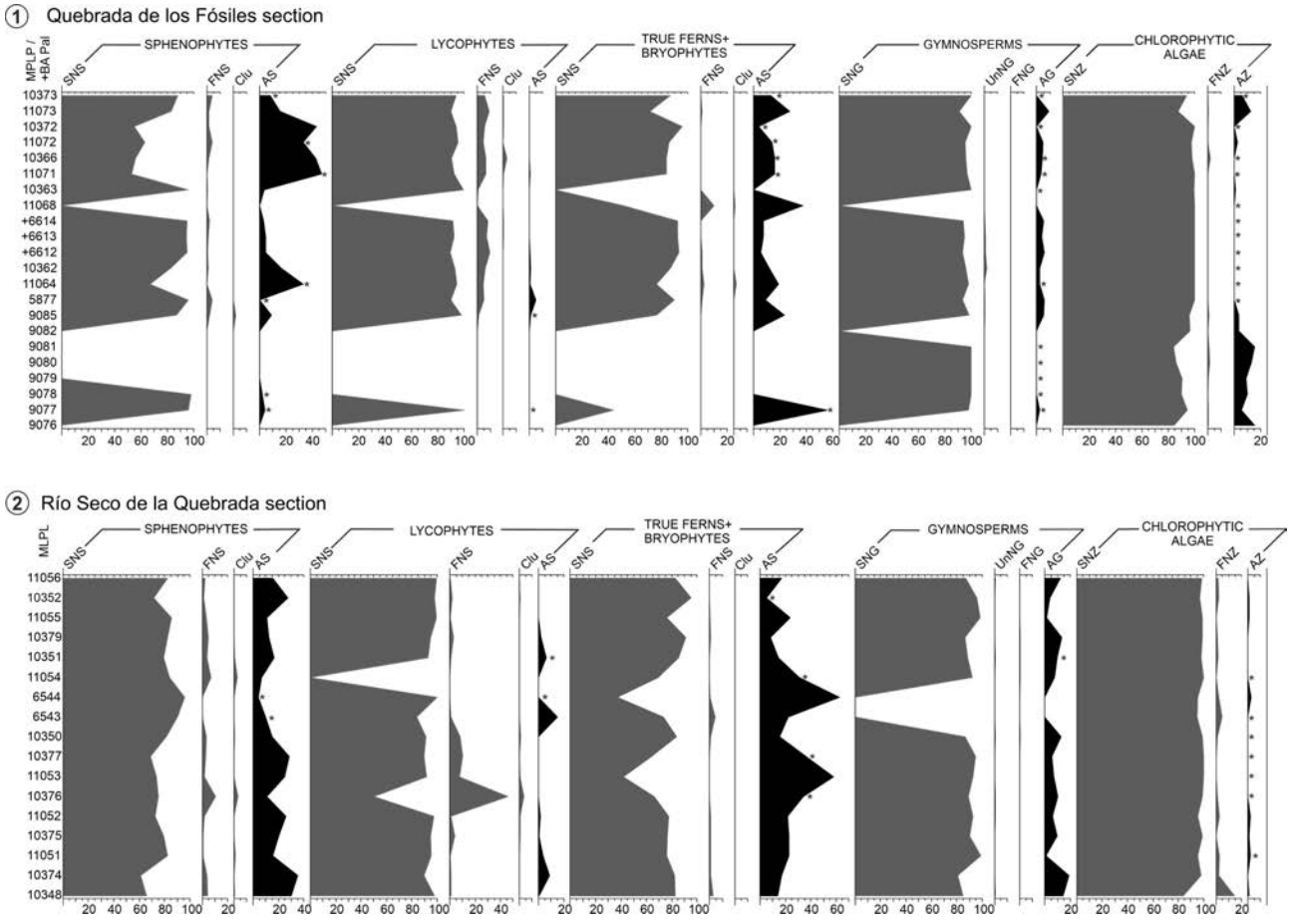

Figure 14. Frequencies of normal and aberrant palynomorph group for each plant lineages recorded in the assemblages of the QdlF Fm in both studied sections. References: **SNS** (Separate normal spores), **FNS** (Fused normal spores: dyad, triad, tetrad), **Clu** (Fused normal spores: cluster), **AS** (Aberrant spores), **SNG** (Separate normal grains), **UnNG** (Unseparated normal grains: dyad, triad, tetrad), **FNG** (Fused normal grains: cluster), **AG** (Aberrant grains), **SNZ** (Separate normal zygospores), **FNZ** (Fused normal zygospores: cluster), **AZ** (Aberrant zygospores).

date, exclusively from the QdlF Fm. The vegetation grew in floodplain facies that laterally intergrade with episodic shallow lacustrine and palustrine deposits associated with incipient developments of paleosols of the high-sinuosity fluvial systems, as suggested by the sedimentological evidence. Coeval extensive events of acid volcanism during deposition of the Puesto Viejo Group —manifested by pyroclastic flow deposits and common to abundant tuffaceous levels— injected large volumes of ash (evidenced by abundant tuffaceous levels) and released volcanic gases (*e.g.*, halocarbons) into the atmosphere that probably induced regional-scale acid rain and ozone holes. Middle Triassic explosive volcanic eruptions potentially influenced climate due to they would have resulted in a strong depletion of the paleo-ozone layer and their harmful ultraviolet radiation affecting the living organisms. The morphological deviations observed in the Puesto Viejo palyno-assemblages are far more extreme than expected due to warming and/or climatic change as a consequence of the regional Choiyoi volcanic activity. Such stressful and adverse conditions (even if not happening catastrophically) affected paleoenvironments that directly influenced the development and composition of plant communities. Environmental stresses in this region could have been imposing intense selective pressures on the plant lineages that persisted there.

The palynoflora is mainly dominated by lycopsid and sphenopsid spores. These plants are excellent stress tolerators. They have had reproductive traits that gave them a competitive advantage and greater reproductive capacity as opportunistic plants in an ecosystem affected repeatedly by pulsed volcanism (Looy *et al.*, 2021).

A lower prevalence of ferns suggests this system was probably experiencing anomalous environmental stresses because otherwise would expect them to proliferate and displace *Pleuromeia*. This genus dominated the Permo-Triassic crisis communities accompanied by pollen malformation and spore tetrad spikes. The low percentages of pollen grains derived from gymnosperms *s.l.* suggest they were selected against this environment by environmental stresses. The scarce participation of pollen grains in the QdlF assemblages suggests that coeval volcanism could strongly affect their development due to woody plants need stable environmental conditions to grow and mature. Thus, selective environmental pressures favor tetrad-producing lycopsids and sphenopsids here over seed plants, as occurred in the Permo-Triassic crises.

The poor diversity of the paleoflora of the QdlF Fm reveals the instability of the environments controlled by tectonic and volcanic activity that occurred when this flora was developing. Its particular evolution could be related to its peripheral position and location on the southwestern edge with respect to the main axis of the Cuyana Basin during Middle Triassic when episodes of extensional rifting occurred in southwestern Gondwana (Monti & Franzese, 2016).

The present study demonstrates the first evidence of unusual rates of teratological features observed in palynological assemblages and also provides signs of mutagenesis in the flora yielded in the Middle Triassic QdlF succession of San Rafael Depocenter. This restricted stratigraphic interval and the manifestation of intense coeval volcanic events and consequent periods of increased atmospheric pollution reveal that plants and/or their cells suffered continuous and/or pulsed intervals of volcanism-induced environmental stress during the QdlF deposition.

The co-occurrence of morphological abnormalities and/or aberrancies in different groups of palynomorphs supports previous analyses that the terrestrial and aquatic population of the QdlF Fm grew inecologically disturbed floodplain environments affected by intermittent volcanic episodes under temperate to warm seasonal semiarid to arid climatic conditions prevailed during the Middle Triassic for southwestern Gondwana, according to the paleogeographic position of Triassic basins of Argentina and the paleoclimatic context (Artabe *et al.*, 2003; Spalletti *et al.*, 2003; Pedernera *et al.*, 2022; Mancuso *et al.*, 2022).

ACKNOWLEDGMENTS

This research has been partially funded by the National Agency for Scientific and Technological Promotion, Argentina (research grants ANPCYT-PICT 2016-0637 PRG, ANPCYT-PICT 2016-0431 PRG, and ANPCYT-PICT 2019-03658 AMZ). Parts of the research that led to the revision of this material were financially supported by the Consejo Nacional de Investigaciones Científicas y Técnicas (CONICET), Argentina (PIP N° 0705 PRG and PIP N° 11220090100605 AMZ). We are deeply indebted to M. Monti for her assistance in the field works, interpretation, and information about the geology of the Puesto Viejo Group, as well as to B. Cariglino for her invaluable assistance in the field. Thanks to A. Moschetti (IANIGLA-CCT-CONICET-Mendoza) for palynological laboratory preparations of samples for light optical microscopy studies, as well as to F. Tricárico who assisted with the scanning electron microscopy. Constructive comments and suggestions by the two reviewers, E. G. Ottone (University of Buenos Aires, Argentina and CONICET) and J. P. Benca

(Museum of Paleontology, University of California-Berkely, U.S.A), greatly helped to improve the final version of the manuscript, thus we are thankful to both.

REFERENCES

Abbink, O. A., Targarona, J., Brinkhuis, H., & Visscher, H. (2001). Late Jurassic to earliest Cretaceous palaeoclimatic evolution of the Southern North Sea. *Global and Planetary Change*, *30*(23), 1–256.

Abbink, O. A., Van Konijnenburg-Van Cittert, J. H. A., Van der Zwan, C. J., & Visscher, H. (2004). A sporomorph ecogroup model for the Northwest European Jurassic-Lower Cretaceous II: Application to an exploration well from the Dutch North Sea. *Netherlands Journal of Geosciences*, *83*(2), 81–91.

Archangelsky, A., Andreis, R. R., Archangelsky, S., & Artabe, A. (1995). Cuticular characters adapted to volcanic stress in a new Cretaceous cycad leaf from Patagonia, Argentina – considerations on the stratigraphy and depositional history ofthe Baquero Formation. *Review of Palaeobotany and Palynology*, *89*(3/4), 213–233.

Artabe, A. E., Morel, E. M., & Spalletti, L. A. (2003). Caracterización de las provincias fitogeográficas triásicas del Gondwana extra-tropical. *Ameghiniana*, *40*(3), 387–405.

Baranyi, V., Rostási, A., Raucsik, B., & Kürschner, W. M. (2019). Palynology and weathering proxies reveal climatic fluctuations during the Carnian Pluvial Episode (CPE) (Late Triassic) from marine successions in the Transdanubian Range (western Hungary). *Global and Planetary Change*, *177*, 157–172.

Bazhina, E. V., Kvitko, O. V., & Muratova, E. N. (2007). Abies sibirica Ledeb. meiosis during microsporogenesis in disturbed forest ecosystems. *Forest Science and Technology*, *3*, 95–100.

Beerling, D. (2007). *The Emerald Planet: How Plants Changed Earth's History*. Oxford University Press, Oxford, United Kingdom.

Benca, J. P., Duijnstee, I. A. P., & Looy, C. V. (2018). UV-B–induced forest sterility: implications of ozone shield failure in Earth's largest extinction. *Science Advances*, *4*(2), e1700618

Benca, J., Duijnstee, I. A. P., & Looy, C. V. (2022). Fossilized pollen malformations as indicators of past environmental stress and meiotic disruption: Insights from modern conifers. *Paleobiology*, *48*(4), 677–710.

Benton, M. J. (2018). Hyperthermal-driven mass extinctions: killing models during the Permian–Triassic mass extinction. *Philosophical Transactions of The Royal Society A Mathematical Physical and Engineering Sciences*, *376*(2130), 20170076.

Black, B. A., Elkins-Tanton, L. T., Rowe, M. C., & Peate, I. U. (2012). Magnitude and consequences of volatile release from the Siberian Traps. *Earth and Planetary Science Letters*, *317–318*, 363–373.

Black, B. A., Lamarque, J.-F., Shields, C. A., Elkinstanton, L. T., & Kiehl, J. T. (2014). Acid rain and ozone depletion from pulsed Siberian Traps magmatism. *Geology*, *42*(1), 67–70.

Cadoux, A., Scillet, B., Bekki, S., Oppenheimer, C., & Druitt, T. H. (2015). Stratospheric ozone destruction by the Bronze Age Minoan eruption (Santorini volcano, Greece). *Scientific Reports 5*, 1–12.

Cariglino, B., Monti, M., & Zavattieri, A. M. (2018). A Middle Triassic macroflora from southwestern Gondwana (Mendoza, Argentina) with typical Northern Hemisphere elements: Biostratigraphic, palaeogeographic and palaeoenvironmental implications. *Review of Palaeobotany and Palynology*, *257*, 1–18.

Chen, J., & Xu, Y. G. (2019). Establishing the link between Permian volcanism and biodiversity changes: Insights from geochemical proxies. *Gondwana Research*, *75*, 68–96.

Chu, D., Dal Corso, J., Shu, W., Song, F., Wignall, P. B., Grasby, S. E., van de Schootbrugge, B., Zong, K., Wu, Y., & Tong, J. (2021). Metal-induced stress in survivor plants following the end–Permian collapse of land ecosystems. *Geology*, *49*(6), 657–661.

Cohen, K. M., Finney, S. C., Gibbard, P. L., & Fan, J.-X. (2013; updated) The ICS International Chronostratigraphic Chart. Episodes 36: 199–204. https://stratigraphy.org/ICSchart/ChronostratChart 2022-02.pdf.

Coturel, E. P., Morel, E. M., & Ganuza, D. (2016). Lycopodiopsids and equisetopsids from the Triassic of Quebrada de los Fósiles Formation, San Rafael Basin, Argentina. *Geobios*, *49*(3), 167–176.

Cui, Y., Li, M., van Soelen, E. E., Peterse, F., & Kürschner, W. M. (2021). Massive and rapid predominantly volcanic CO2 emission during the end–Permian mass extinction. *PNAS*, *118*(37). doi: 10.1073/pnas.2014701118.

Del Fueyo, G. M., Guignard, G., Villar de Seoane, L., & Archangelsky, S. (2013). Leaf Cuticle Anatomy and the Ultrastructure of Ginkgoites ticoensis Archang. from the Aptian of Patagonia. *International Journal of Plant Sciences*, *174*(3), 406–424.

De Storme, N., & Geelen, D. (2013). The impact of environmental stress on male reproductive development in plants: biological processes and molecular mechanisms. *Plant, Cell and Environment 37*(1), 1–18.

Domeier, M., Van der Voo, R., Tomezzoli, R. N., Tohver, E., Hendriks, B. W., Torsvik, T. H., Vizán, H., & Domínguez, A. (2011). Support for an "A-type" Pangea reconstruction from high-fidelity Late Permian and Early to Middle Triassic paleomagnetic data from Argentina. *Journal of Geophysical Research*, *116*(B12), 1–26.

Dzyuba, O. F. (1998). Paleoecological reconstructions and quality angiosperm pollen grains in stressful environments. *Paleontological Journal*, *32*, 97–101.

Fijałkowska-Mader, A. (2020). Impact of the environmental stress on the Late Permian pollen grains from Zechstein deposits of Poland. In J. Guex, W. B. Miller Jr., & J. S. Torday (Eds.), *Morphogenesis, environmental stress and reverse evolution* (pp. 23–35). Springer, Cham, Switzerland.

Font, E., Chen, J., Regelous, M., Regelous, A., & Adatte, T. (2022). Volcanic origin of the mercury anomalies at the Cretaceous-Paleogene transition of Bidart, France. *Geology*, *50*(2), 142–146.

Foster, C. B., & Afonin, S. A. (2005). Abnormal pollen grains: an outcome of deteriorating atmospheric conditions around the Permian–Triassic boundary. *Journal of the Geological Society*, *162*(4), 653–659.

Gnaedinger, S., Cariglino, B., Zavattieri, A. M., Monti, M., & Gutiérrez, P. R. (2020). *Neoarthropitys gondwanaensis* gen. nov. et sp. nov. from the Middle Triassic of Gondwana: an intermediate stage in the anatomical trend of Equisetalean stems. *Review of Palaeobotany and Palynology*, *282*, 104298.

González Díaz, E. F. (1964). Rasgos geológicos y evolución geomorfológica de la Hoja 27d, San Rafael y zona occidental vecina (Provincia de Mendoza). *Revista de la Asociación Geológica Argentina*, *19*(3), 151–188.

González Díaz, E. F. (1972). Descripción geológica de la Hoja 27d, San Rafael, provincia de Mendoza. *Carta Geológico-Económica de la República Argentina. Escala 1:200.000. Boletín 132, 143 p., Servicio Nacional Minero Geológico.*

Grasby, S. E., Liu, X., Yin, R., Ernst, R. E., & Chen, Z. (2020). Toxic mercury pulses into late Permian terrestrial and marine environments. *Geology*, *48*(8), 830–833

Grasby, S. E., Sanei, H., Beauchamp, B., & Chen, Z. (2013). Mercury deposition through the Permo–Triassic biotic crisis. *Chemical Geology*, *351*, 209–216.

Grasby, S. E., Them, T. R., II, Chen, Z., Yin, R., & Ardakani, O. H. (2019). Mercury as a proxy for volcanic emissions in the geologic record.

Earth-Science Reviews, *196*, 102880.

Gupta, M., & Devi, S. (1994). Chronic toxicity of cadmium in *Pteris vittata*, a roadside fern. *Ecotoxicology*, *3*, 235–247.

Gutiérrez, P. R., & Zavattieri, A. M. (2021). New Middle Triassic pollen taxa of the San Rafael Basin, Mendoza Province, Argentina. *Ameghiniana*, *57*(1), 1–22.

Hochuli, P. A., Schneebeli-Hermann, E., Mangerud, G., & Bucher, H. (2017). Evidence for atmospheric pollution across the Permian–Triassic transition. *Geology*, *45*(12), 1123–1126.

Irmis, R. B., Mundil, R., Mancuso, A. C., Carrillo-Briceño, J. D., Ottone, E. G., & Marsicano, C. A. (2022). South American Triassic geochronology: Constraints and uncertainties for the tempo of Gondwanan non-marine vertebrate evolution. *Journal of South American Earth Sciences*, *116*, 103770.

Kay, S. M., Ramos, V. A., Mpodozis, C., & Sruoga, P. (1989). Late Paleozoic to Jurassic silicic magmatism at the Gondwana margin: analogy to middle Proterozoic in North America. *Geology*, *17*(4), 324–328.

Kelber, K. P., & van Konijnenburg-van Cittert, J. H. A. (1998). *Equisetites arenaceus* from the Upper Triassic of Germany with evidence for reproductive strategies. *Review of Palaeobotany and Palynology*, *100*(1–2), 1–26.

Kerp, H. (1990). The Study of Fossil Gymnosperms by Means of Cuticular Analysis. *Palaios*, *5*(6), 548–569.

Kleiman, L. E., & Japas, M. S. (2009). The Choiyoi Volcanic Province at 34°S–36°S (San Rafael, Mendoza, Argentina): implications for the late Palaeozoic evolution of the southwestern margin of Gondwana. *Tectonophysics*, *473*(3-4), 283–299.

Kleiman, L. E., & Salvarredi, J. A. (2001). Petrología, geoquímica e implicancias tectónicas del volcanismo Triásico (Formación Puesto Viejo), Bloque de San Rafael, Mendoza. *Revista de la Asociación Geológica Argentina*, *56*(4), 559–570.

Kokogián, D. A., Spalletti, L. A., Morel, E. M., & Artabe, A. E. (1999). Los depósitos continentales triásicos. In: R. Caminos (Ed.), *Geología Argentina* (pp. 377–398). Instituto de Geología y Recursos Minerales.

Kokogián, D. A., Spalletti, L. A., Morel, E. M., Artabe, A. E., Martínez, R. N., Alcober, O. A., Milana, J. P., & Zavattieri, A. M. (2001). Estratigrafía del Triásico argentino. In A. E. Artabe, E. M. Morel, A. B. Zamuner (Eds.), *El Sistema Triásico en la Argentina* (pp. 23–54).

Koti, S., Reddy, K. R., Reddy, V. R., Kakani, G., & Zhao, D. L. (2005). Interactive effects of carbon dioxide, temperature, and ultraviolet-B radiation on soy bean (Glycine max L.) flower and pollen morphology, pollen production, germination, and tube lengths. *Journal of Experimental Botany*, *56*(412), 725–736.

Koti, S., Reddy, K. R., Reddy, V. R., Kakani, G., Zhao, D. L., & Gao, W. (2007). Effects of carbon dioxide, temperature and ultraviolet-B radiation and their interactions on soybean (*Glycine max* L.) growth and development. *Environmental and Experimental Botany*, *60*(1), 1–10.

Kürschner, W. M., Batenburg, S. J., & Mander, L. (2013). Aberrant Classopollis pollen reveals evidence for unreduced (2n) pollen in the conifer family Cheirolepidiaceae during the Triassic–Jurassic transition. *Proceedings of the Royal Society of London B*, *280*(1768), 20131708.

Kustatscher, E., Van Konijnenburg-van Cittert, J. H. A., Bauer, K., Butzmann, R., Meller, B., & Fischer, T. C. (2012). A new flora from the upper Permian of Bletterbach (Dolomites, N Italy). *Review of Palaeobotany and Palynology*, *182*, 1–13.

Kutterolf, S., Hansteen, T. H., Appel, K., Freundt, A., Krüger, K., Pérez, W., & Wehrmann, H. (2013). Combined bromine and chlorine release from large explosive volcanic eruptions: A threat to stratospheric ozone? *Geology*, *41*, 707–710.

Lindström, S., McLoughlin, S., & Drinnan, A. D. (1997). Intraspecific variation of taeniate bisaccate pollen within Permian Glossopterid sporangia, from the Prince Charles Mountains, Antarctica. *International Journal of Plant Sciences*, *158*(5), 673–684.

Lindström, S., Sane, H., van de Schootbrugge, B., Pedersen, G. K., Lesher, C. E., Tegner, C., Heunisch, C., Dybkjær, K., & Outridge, P. M. (2019). Volcanic mercury and mutagenesis in land plants during the end–Triassic mass extinction. *Science Advances*, *5*(10), doi: 10.1126/sciadv.aaw4018.

Lindström, S., van de Schootbrugge, B., Hansen, K. H., Pedersen, G. K., Alsen, P., Thibault, N., Dybkjær, K., Bjerrum, C. J., & Nielsen, L. H. (2017). A new correlation of Triassic–Jurassic boundary successions in NW Europe, Nevada and Peru, and the Central Atlantic Magmatic Province: a time-line for the end–Triassic mass extinction. *Palaeogeography, Palaeoclimatology, Palaeoecology*, *478*, 80–102.

Llambías, E. J., Kleiman, L. E., & Salvarredi, J. A. (1993). El Magmatismo gondwánico. In V. A. Ramos (Ed.), *Geología y Recursos Naturales de Mendoza. XII Congreso Geológico Argentino y II Congreso de Exploración de Hidrocarburos. Relatorio*, *1*(6), 53–64.

Llambías, E. J., & Sato, A. M. (1995). El batolito de Colangüil: Transición entre orogénesis y anorogénesis. *Revista de la Asociación Geológica Argentina*, *50*(1), 111–131.

Lomax, B. H., Fraser, W. T., Sephton, M. A., Callaghan, T. V., Self, S., Harfoot, M., Pyle, J. A., Wellman, C. H., & Beerling, D. J. (2008). Plant spore walls as a record of long-term changes in ultraviolet-B radiation. *Nature Geoscience*, *1*(9), 592–596.

Looy, C. V., Collinson, M. E., van Konijnenburg-van Cittert, J. H. A., Visscher, H., & Brain, A. P. R. (2005). The ultrastructure and botanical affinity of end–Permian spore tetrads. *International Journal of Plant Sciences*, *166*(5), 875–887.

Looy, C. V., Twitchett, R. J., Dilcher, D. L., Van Konijnenburg-van Cittert, J. H., & Visscher, H. (2001). Life in the end–Permian dead zone. *Proceedings of the National Academy of Sciences USA*, *98*(14), 7879–7883.

Looy, C. V., van Konijnenburg-van Cittert, J. H. A., & Duijnstee, I. A. P. (2021). Proliferation of Isoëtalean Lycophytes during the Permo–Triassic biotic crises: A proxy for the state of the Terrestrial Biosphere. *Frontiers in Earth Science*, *9*. doi: 10.3389/feart.2021.615370.

López Gamundí, O., Álvarez, L., Andreis, R., Bossi, G., Espejo, I., Fernándes Seveso, E., Legarreta, L., Kokogián, D., Limarino, O., & Sesarego, H. (1989). Cuencas Intermontanas. In G. Chebli & L. Spalletti (Eds.), *Cuencas Sedimentarias Argentinas. Serie Correlación Geológica*, *6*, 123–167.

Mancuso, A. C., Horn, B. L. D., Benavente, C. A., Schultz, C. L., & Irmis, R. B. (2021). The Paleoclimatic Context for South American Triassic Vertebrate Evolution. *Journal of South American Earth Sciences*, *110*, 103321.

Mancuso, A. C., Irmis, R. B., Pedernera, T. E., Gaetano, L. C., Benavente, C. A., & Breeden III, B. T. (2022). Paleoenvironmental and Biotic Changes in the Late Triassic of Argentina: Testing Hypotheses of Abiotic Forcing at the Basin Scale. *Frontiers in Earth Science*, *10*. https://doi.org/10.3389/feart.2022.883788.

Marshall, J. E. A., Lakin, J., Troth, I., & Wallace-Johnson, S. M. (2020). UV-B radiation was the Devonian-Carboniferous boundary terrestrial extinction kill mechanism. *Science Advances*, *6*(22), eaba0768.

Martínez, L. C. A., Artabe, A. E., & Archangelsky, S. (2020). Studies of the leaf cuticle fine structure of *Zuberia papillata* (Townrow) Artabe 1990 from Hoyada de Ischigualasto (Upper Triassic), San Juan Province, Argentina. *Review of Palaeobotany and Palynology*, *281*, 104272.

McGhee, G. R. Jr., Clapham, M. E., Sheehan, P. M., Bottjer, D. J., & Droser, M. L. (2013). A new ecological-severity ranking of major Phanerozoic biodiversity crises. *Palaeogeography, Palaeoclimatology, Palaeoecology*, *370*, 260–270.

Mičieta, K., & Murín, G. (1996). Microspore analysis for genotoxicity of a polluted environment. *Environmental and Experimental Botany*, *36*(1), 21–27.

Monti, M. (2015). *Tectónica, volcanismo y sedimentación en la cuenca triásica del Grupo Puesto Viejo (Triásico Medio–Superior), provincia de Mendoza.* (Tesis Doctoral, Facultad de Ciencias Naturales y Museo, Universidad Nacional de La Plata, La Plata). Available from http://sedici.unlp.edu.ar/handle/10915/44602.

Monti, M., & Franzese, J. R. (2016). Análisis tectonoestratigráfico del Grupo Puesto Viejo (San Rafael, Argentina): evolución de un rift continental triásico. Latin American *Journal of Sedimentology, Basin Analysis*, *23*(1), 1–33.

Monti, M., & Franzese, J. R. (2019). Triassic continental oblique rifting controlled by Paleozoic structural grain: The Puesto Viejo Basin, western Argentina. *Journal of South American Earth Sciences*, *95*, 102–240.

Monti, M., Sato, A. M., & Franzese, J. R. (2018). Edad del rifting Triásico en la cuenca de Puesto Viejo (U-Pb 243.9±2 Ma), San, Rafael, provincia de Mendoza. *Acta XVI Reunión Argentina de Sedimentología* (p. 81), Río Negro, Argentina.

Nowak, H., Schneebeli-Hermann, E., & Kustatscher, E. (2019). No mass extinction for land plants at the Permian–Triassic transition. *Nature Communications*, *10*(1), 384.

Osipov, S., Stenchikov, G., Tsigaridis, K., Le Grande, A. N., & Bauer, S. E. (2020). The role of the SO2 radiative effect in sustaining the volcanic winter and soothing the Toba impact on climate. *Journal of Geophysical Research. Atmospheres*, *125*, e2019JD031726.

Ottone, E. G., & García, G. B. (1991). A Lower Triassic miospore assemblage from the Puesto Viejo Formation, Argentina. *Review of Palaeobotany and Palynology*, *68*(3–4), 217–232.

Ottone, E. G., Monti, M., Marsicano, C. A., de La Fuente, M. S., Naipauer, M., Armstrong, R., & Mancuso, A. C. (2014). A new Late Triassic age for the Puesto Viejo Group (San Rafael depocenter, Argentina): SHRIMP U–Pb zircon dating and biostratigraphic correlations across southern Gondwana. *Journal of South American Earth Sciences*, *56*, 186–199.

Paterson, N. W., Mangerud, G., Cetean, C. G., Mørk, A., Lord, G. S., Klausen, T., & Mørkved, P. T. (2016). A multidisciplinary biofacies characterisation of the Late Triassic (Late Carnian–Rhaetian) Kapp Toscana Group on Hopen, Arctic Norway. *Palaeogeography, Palaeoclimatology, Palaeoecology*, *464*, 16–42.

Paterson, N. W., Mangerud, G., & Mørk, A. (2017). Late Triassic (early Carnian) palynology of shallow stratigraphical core 7830/5-U-1, offshore Kong Karls Land, Norwegian Arctic. *Palynology*, *41*(2), 230–254.

Payne, R. J., & Egan, J. (2019). Using palaeoecological techniques to understand the impacts of past volcanic eruptions. *Quaternary International*, *499*(B), 278–289.

Pedernera, T. E., Mancuso, A. C., & Ottone, E. G. (2022). Triassic paleoclimate and paleofloristic trends of southwestern Gondwana (Argentina). *Journal of South American Earth Sciences*, *116*, 103852.

Pott, C., Krings, M., & Kerp, H. (2008). The Carnian (Late Triassic) flora from Lunz in Lower Austria: Paleoecological considerations. *Palaeoworld*, *17*(3/4), 172–182.

Rabe, E. W., & Haufler, C. H. (1992). Incipient polyploid speciation in the maidenhair fern (Adiantum pedatum, Adiantaceae)? *American Journal of Botany*, *79*(6), 701–707.

Racki, G. (2020). Volcanism as a prime cause of mass extinctions: Retrospectives and perspectives. In T. Adatte, D. P. G. Bond, & G. Keller (Eds.), *Mass Extinctions, Volcanism, and Impacts: New Developments*. Geological Society of America Special Paper 544, p. 1–34.

Ram-Awatar (2011). Occurrence of spore tetrads in the Pali sediments of South Rewa Basin, India and their climatic inference. *The Palaeobotanist*, *60*(2), 363–368.

Ries, G., Heller, W., Puchta, H., Sandermann, H., Seidlitz, H. K., & Hohn, B. (2000). Elevated UV-B radiation reduces genome stability in plants. *Nature*, *406*, 98–101.

Rocha-Campos, A. C., Basei, M. A. S., Nutman, A. P., Kleiman, L., Varela, R., Llambías, E., Canile, F. M., & Rosa, O. C. R. da (2011). 30 million years of Permian volcanism recorded in the Choiyoi igneous Province (W Argentina) and their source for younger ash fall deposits in the Paraná Basin: SHRIMP U-Pb zircon geochronology evidence. *Gondwana Research*, *19*(2), 509–523.

Ruffo Rey, L. (2021). Vegetation dynamics of Cerro de Las Cabras Formation (Middle Triassic) from palynological assemblages and the Eco-Guild model: New paleoenvironmental and paleoclimatic interpretations. *Journal of South American Earth Sciences*, *112*(2), 103629.

Sato, A. M., Llambías, E. J., Basei, M. A. S., & Castro, C. E. (2015). Three stages in the Late Paleozoic to Triassic magmatism of southwestern Gondwana, and the relationships with the volcanogenic events in coeval basins. *Journal of South American Earth Sciences*, *63*, 48–69.

Saxena, A., Singh, K. J., Murthy, S., Chandra, S., & Goswami, S. P. (2015). Spore tetrads, possible indicators of intense climatic regimes: case study from an early Permian stratum of Singrauli Coalfield, Son-Mahanadi Basin, India. *Geological Magazine*, *153*(3), 426–437.

Shen, J., Yin, R., Algeo, T. J., Svensen, H. H., & Schoepfer, S. D. (2022). Mercury evidence for combustion of organic-rich sediments during the end–Triassic crisis. *Nature Communications*, *13*(1), 1–8.

Spalletti, L. A. (1994). Evolución de los ambientes fluviales en el Triásico de la Sierra Pintada (Mendoza, Argentina): análisis sobre la influencia de controles intrínsecos y extrínsecos al sistema depositacional. *Revista de la Asociación Argentina de Sedimentología*, *1*(2), 125–142.

Spalletti, L. A., Artabe, A. E., & Morel, E. M. (2003). Geological Factors and Evolution of Southwestern Gondwana Triassic Plants. *Gondwana Research*, *6*(1), 119–134.

Spalletti, L. A., & Limarino, C. L. (2017). The Choiyoi magmatism in south western Gondwana: implications for the end–Permian mass extinction - a review. *Andean Geology*, *44*(3), 328–338.

Stipanicic, P. N., González Díaz, E. F., & Zavattieri, A. M. (2007). Grupo Puesto Viejo nom. transl. por Formación Puesto Viejo González Díaz (1994, 1967): nuevas interpretaciones paleontológicas, estratigráficas y cronológicas. *Ameghiniana*, *44*(4), 759–761.

Stukins, S. (2022). Is aberrancy a reliable indicator for major paleoclimatic disturbance? *Palaios*, 37(5), 145–149.

Sun, Y. D., Joachimski, M. M., Wignall, P. B., Yan, C. B., Chen, Y. L., Jiang, H. S., Wang, L. D., & Lai, X. L. (2012). Lethally hot temperatures during the Early Triassic Greenhouse. *Science*, *338*(6105), 366–370.

Tassi, L. V., Monti, M., Gallego, O. F., Zavattieri, A. M., & Lara, M. B. (2013). The first spinicaudatan (Crustacea: Diplostraca) from Permo–Triassic continental sequences of South America and its palaeoecological context. *Alcheringa, 37*(2), 189–201.

Taylor, E. L., Taylor, T. N., & Krings, M. (2009). *Paleobotany: The Biology and Evolution of Fossil Plants* (pp. 1252). Academic Press, Massachusetts.

Tiwari, R. S., & Meena, K. L. (1989). Abundance of spore tetrads in the Early Triassic sediments of India and their significance. *The*

Palaeobotanist, *37*(2), 210–214.

Vázquez, M. S. (2013). *Palinología de la Formación Quebrada de los Fósiles, Pérmico-Triásico de San Rafael, provincia de Mendoza.* (Tesis de Licenciatura, Facultad de Ciencias Exactas y Naturales, Universidad de Buenos Aires, Buenos Aires). (unpublished).

Visscher, H., Looy, C. V., Collinson, M. E., Brinkhuis, H., van Konijnenburg-van Cittert, J. H. A., Kürschner, W. M., & Sephton, M. A. (2004). Environmental mutagenesis during the end–Permian ecological crisis. *Proceedings of the National Academy of Sciences*, *101*(35), 12952–12956.

Visscher, H., Sephton, M. A., & Looy, C. V. (2011). Fungal virulence at the time of the end–Permian biosphere crisis?. *Geology*, *39*(9), 883–886.

Ward, P. L. (2009). Sulfur dioxide initiates global climate change in four ways. *Thin Solid Films*, *517*(11), 3188–3203.

Wignall, P. B. (2001). Large igneous provinces and mass extinctions. *Earth-Science Reviews*, *53*(1-2), 1–33.

Wignall, P. B. (2005). The Link between Large Igneous Province Eruptions and Mass Extinctions. *Elements*, *1*(5), 293–297.

Williams, S. N., Schaefer, S. J., Calvache, M. L., & Lopez, D. (1992). Global carbon dioxide emission to the atmosphere by volcanoes. *Geochimica et Cosmochimica Acta*, *56*(4), 1765–1770.

Yin, H., Jiang, H., Xia, W., Feng, Q., Zhang, N., & Shen, J. (2014). The end–Permian regression in South China and its implication on mass extinction. *Earth-Science Reviews*, *137*(2), 19–33.

Zavattieri, A. M., Gutiérrez, P. R., & Monti, M. (2020). Middle Triassic freshwater green algae and fungi of the Puesto Viejo Basin, central-western Argentina: Palaeoenvironmental implications. *Alcheringa*, *44*(3), 430–459.

doi: 10.5710/AMGH.24.01.2023.3533

Submitted: 25 July 2022
Accepted: 24 January 2023
Published: 31 March 2023